Intelligent Oncology 1 (2025) 139–159

Contents lists available at ScienceDirect

Intelligent Oncology

journal homepage: www.keaipublishing.com/en/intonc/

Review

Computational pathology: A comprehensive review of recent developments in digital and intelligent pathology

Qinqin Huang[a], Shen'ao Wu[a], Zhenkai Ou[a], Yi Gao[a,b,c,*]

[a] School of Biomedical Engineering, Shenzhen University Medical School, Shenzhen University, Shenzhen Guangdong 518037, China
[b] Guangdong Provincial Key Laboratory of Mathematical and Neural Dynamical Systems, Dongguan Guangdong 523000, China
[c] Marshall Laboratory of Biomedical Engineering, Shenzhen Guangdong 518060, China

ARTICLE INFO

Keywords:
Computational pathology
Generative AI
Whole-slide image
Pathology image analysis
Pathology foundation models

ABSTRACT

Computational pathology, a field at the intersection of computer science and pathology, leverages digital technology to enhance diagnostic accuracy and efficiency. With the digitization of pathology and the development of artificial intelligence, computational pathology has made significant strides in the automatic analysis of pathology images, including pathological structure segmentation, tumor classification, and prognosis analysis. Driven by large-scale datasets and advanced methods, computational pathology is moving toward building foundation models to reach more general applications. Generative methods provide a new perspective on addressing challenges in computational pathology. However, challenges in data security and model reliability, reproducibility, and clinical application remain. This review outlines the evolution of computational pathology from pathology slide digitization to pathology image analysis, consolidates the development of foundation and generative models in computational pathology, and discusses the key challenges that persist. Finally, we introduce some rising techniques for precision pathology.

1. Introduction

Computational pathology integrates advanced digitization and analysis technologies into the field of pathology, enhancing research and clinical diagnosis. The digitization of pathology slide images is a process that converts pathological slides into whole-slide images (WSIs). This can preserve the integrity of the original pathology data and enable computational analysis.

Due to the large size of gigapixel images, pathology image analysis suffers from challenges such as memory constraints and processing speed. To manage these large images, tiling divides them into smaller, manageable segments, enabling efficient processing and reducing memory demands. Additionally, graphics processing units leverage parallel computation, accelerating tasks such as segmentation and classification by distributing operations across multiple cores.

The continuous development of image-processing algorithms has been pivotal to the evolution of computational pathology since the 1980s. In the 2010s, the use of machine learning in computational pathology began to emerge.[1,2] The success of AlexNet in 2012 marked a breakthrough in deep learning for image analysis, driving its application in pathology image analysis, including in cell segmentation, tumor detection, tissue classification, and prognostic prediction. Different from predictive models, generative models create synthetic data, expanding the scope of deep learning applications in pathology and promoting the performance of deep

* Corresponding author.
E-mail address: gaoyi@szu.edu.cn (Y. Gao).

https://doi.org/10.1016/j.intonc.2025.03.004
Received 11 October 2024; Received in revised form 7 March 2025; Accepted 7 March 2025
Available online 22 March 2025
2950-2616/© 2025 The Author(s). Publishing services by Elsevier B.V. on behalf of KeAi Communications Co. Ltd. This is an open access article under the CC BY license (http://creativecommons.org/licenses/by/4.0/).

learning-based models. Recently, advances in artificial intelligence (AI) have provided a robust technical foundation for computational pathology. Through deep learning algorithms, computers can learn and extract features from a large dataset of pathology images, enabling automated analysis.

The volume of pathology data is growing rapidly. This growth was initiated by the Cancer Genome Atlas program led by the National Cancer Institute of United States , which released a vast amount of pathology images and genetic data.[3] With such growth, the application of big data technology has become increasingly important. In big data technology, massive amounts of data can be stored, managed, and analyzed to discover the relationships and patterns hidden in the data. Furthermore, cloud computing simplifies the storage, sharing, and computation of pathology data, facilitating cross-organizational collaboration and research.

The development of precision medicine is also one of the key driving factors of computational pathology. Precision medicine emphasizes the development of personalized treatment plans based on an individual's genetic, environmental, and lifestyle factors. Pathology, as an important component of precision medicine, requires efficient and accurate tools for analyzing pathology images. Computational pathology provides comprehensive pathology information by integrating pathology images, genomic data, and clinical data, helping to achieve accurate diagnosis and treatment. The emergence of novel techniques and methods can accelerate the development of precision medicine, such as 3D pathology, omics, and multimodality models.

Therefore, this review summarizes the development of the main directions of computational pathology in precision medicine, including digital pathology images, pathology image preprocessing, pathology image analysis, and synthetic pathology data. Moreover, with foundation models emerging, their applications in pathology are condensed in this review. Finally, we discuss some ongoing challenges and outline several emerging directions.

2. WSI acquisition and display

WSI acquisition involves several stages, including slide preparation, staining, microscopy, scanning, and stitching. Additionally, various applications support WSI viewing and enable algorithms for further analysis. The whole process is summarized in Figure 1A.

2.1. Slide preparation

Slide preparation is a fundamental step in ensuring an accurate diagnosis. Tissue samples are obtained from patients through surgery or biopsy. These samples are processed using various methods, including formalin-fixed paraffin-embedded sections, frozen sections, and smearing. The formalin-fixed paraffin-embedded preserves tissue by fixing it in formalin, embedding it in paraffin, and sectioning it for long-term storage and histological analysis. In frozen sections, tissue is rapidly frozen and sectioned to preserve molecular integrity, which allows it to be utilized in intraoperative diagnosis, though it may suffer from cold-induced damage. In smearing, fluid samples are spread on slides before undergoing fixation and staining, making this process suitable for blood and bone marrow.

2.1.1. Staining

Staining is a key procedure in manifesting tissue structure. The principle of staining is based on the affinity of different tissues or cells to specific dyes. Various staining techniques substantially enhance the visualization of tissue details and assist in more precise pathology analysis (Figure 1B).

The most common staining method is hematoxylin-eosin (H&E) staining wherein hematoxylin binds with cell nuclei and eosin binds with the cytoplasm, showing an overall blue-pinkish color. While H&E provides a clear structural view of the cells and tissues, it does not have the molecular specificity for certain differential diagnoses.

In contrast, immunohistochemistry (IHC) and immunofluorescence are groups of staining methods with high specificity to detect protein expression in tissue sections based on the mechanism of antibody–antigen binding. Antibodies are conjugated with enzymes in IHC or fluorescent dyes in immunofluorescence to detect and visualize specific antigens. In IHC, enzymes catalyze a color change through an enzyme–substrate reaction. IHC offers stable markers for routine histological studies. However, IHC is limited by the narrow color range of its enzymatic reactions, which restricts its ability to support multiplex staining. Immunofluorescence uses fluorescent dyes conjugated to antibodies, with multispectral excitation enabling precise quantitative analysis and multiplex staining. It has lower toxicity than IHC and is suitable for dynamic live cell imaging to study cell behavior. However, it is prone to photobleaching, limiting repeated imaging.

Additionally, there are special staining techniques, such as Masson's trichrome, periodic acid–Schiff (PAS) staining, and Jones' methenamine silver staining. These methods rely on the affinity of specific tissues or cells for certain dyes, targeting different tissue components or pathological conditions to highlight and identify specific structures or changes.

2.1.2. Microscopy

For H&E and IHC images, bright-field microscopy is typically used for observation. Here, visible light transmits through the sample for imaging. Fluorescence imaging has advanced with techniques such as wide-field, confocal, light sheet, and super-resolution microscopy, enabling higher resolutions and multichannel imaging. Wide-field microscopy captures large sample areas with uniform illumination, which is ideal for quick fluorescent marker observation. However, it suffers from out-of-focus blur and background noise, reducing contrast and resolution. In contrast, confocal microscopy uses a laser to exclude out-of-focus signals, enhancing contrast and resolution for thicker samples but at a slower imaging speed. Light sheet microscopy excites specific regions

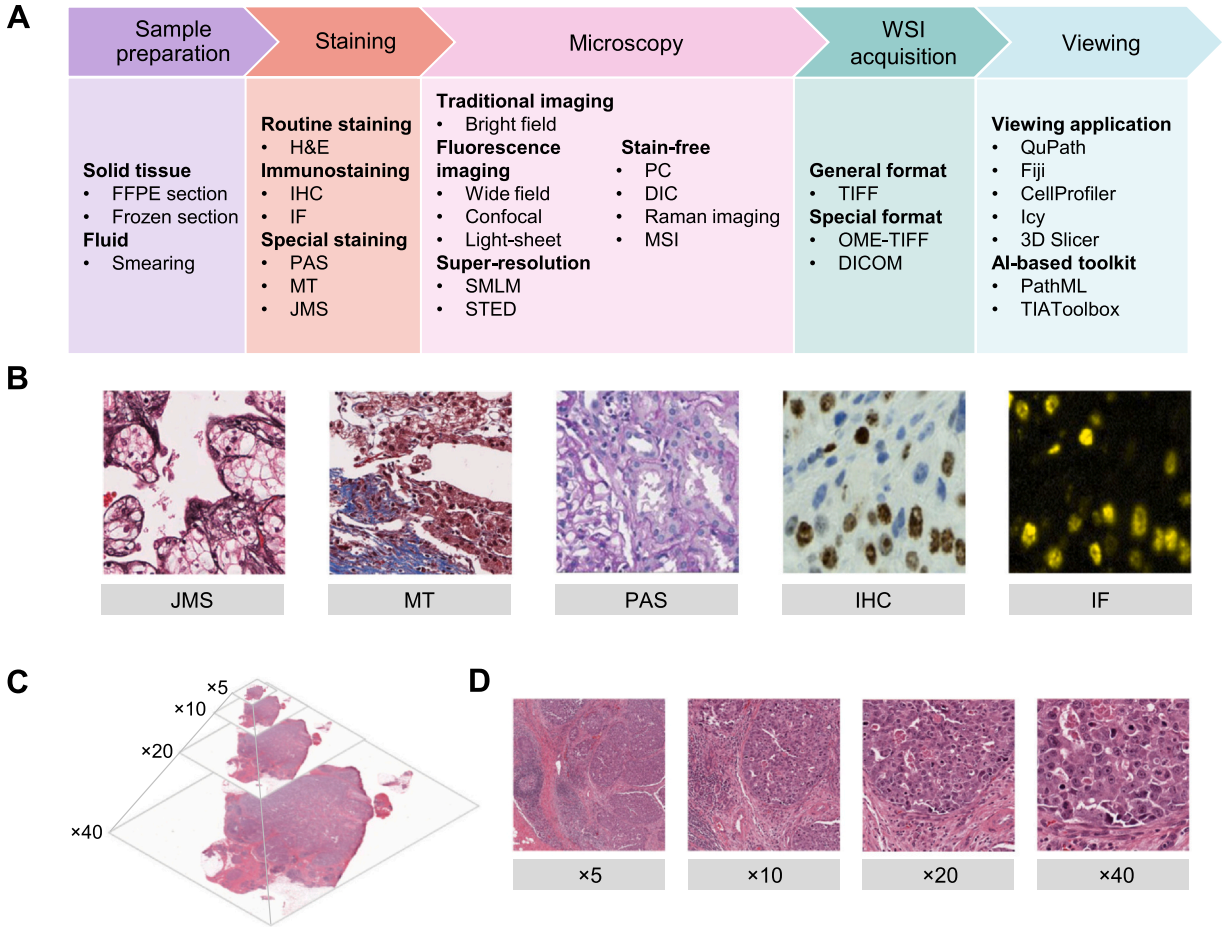


Figure 1. Whole-slide image (WSI) digitization procedure. Figure 1A illustrates the whole process of WSI digitization composed of sample preparation, staining, microscopy, WSI acquisition, and viewing. Figure 1B illustrates various staining types, with permission from the publishers, including the Springer Nature[4,5] and the American Chemical Society.[6] Figure 1C is a WSI pyramid. Figure 1D illustrates different magnifications in WSI. Abbreviations: 1. FFPE: formalin-fixed paraffin-embedded 2. H&E: hematoxylin and eosin 3. IHC: immunohistochemistry 4. IF: immunofluorescence 5. MT: Masson's trichrome 6. PAS: periodic acid-Schiff 7. JMS: Jones' methenamine silver 8. SMLM: single molecule localization microscopy 9. STED: stimulated emission depletion microscopy 10. PC: phase contrast 11. DIC: differential interference contrast 12. MSI: mass spectrometry imaging 13. TIFF: tagged image file format 14. OME-TIFF: open microscopy environment TIFF 15. DICOM: digital imaging and communications in medicine.

with a thin light sheet, scanning layer by layer for 3D data, though resolution is limited by diffraction. Super-resolution techniques (such as stimulated emission depletion microscopy and single molecule localization microscopy) surpass the diffraction limit, providing higher resolutions for detailed observations.[7]

Meanwhile, stain-free microscopic techniques are rapidly advancing. Early differential imaging techniques (e.g., phase-contrast microscopy and differential interference contrast microscopy) enable the observation of fine structural contours in transparent samples and live cells. Recent advancements in Raman imaging and mass spectrometry imaging have enabled the precise mapping of molecular components without the need for traditional staining methods. In Raman imaging, light from a Raman laser interacts with cellular molecules, exciting them to produce specific spectral features. By detecting these spectral signals and combining spatial information, Raman imaging provides detailed information on the chemical composition and molecular structure of the sample.[8] Mass spectrometry imaging extracts ions from the surface of the sample using specific techniques and analyzes their mass and abundance with a mass spectrometer, revealing the composition of the sample.[9]

2.2. WSI acquisition

The pathology slides prepared above are sent to a high-resolution scanner. Modern scanners can achieve image resolutions below 0.2 microns per pixel with a total magnification of 400 times using a ×10 eyepiece and a ×40 objective, as illustrated in Figure 1C and 1D. The camera of a scanner can typically capture an image of approximately 2000 × 2000 pixels within a single field of view. This image is referred to as a "tile." To acquire the entire tissue image from a pathology slide, multiple tiles must be scanned and then stitched together to form a large WSI. Image stitching mainly uses registration methods to extract and match feature points, calculate the transformation matrix, and seamlessly fuse the images through spatial transformation.[10]

For the entire 15 × 15 mm sample range, up to tens of billions of pixels can be obtained. The file size ranges from hundreds of megabytes to several gigabytes for a single image. Therefore, with such an ultra-high pixel count, WSI requires special storage formats and viewing solutions.

Rather than the formats commonly used for photo images, the tagged image file format (TIFF) is a more suitable choice for storing such large WSIs. Indeed, most scanner manufacturers use WSI formats based on the TIFF image format and its variants, such as BigTIFF and GeoTIFF. These formats not only support the reading of any area but also store multiple magnification and down-sampling multiples of images (×5, ×10, ×20, ×40) in a pyramid structure. It is worth mentioning that lossy compression, which is often taboo for radiology images, is widely used in pathology image storage due to the huge amount of pathology images. It is precisely because of the sufficient compression rate of lossy compression that remote pathology consultation becomes possible.

However, the current WSI format lacks a unified standard, which affects its interoperability and storage efficiency. To address this challenge, the Open Microscopy Environment TIFF (OME-TIFF)[11] and Digital imaging and communications in medicine[12] aim to unify WSI storage formats. OME-TIFF was developed by the OME organization and supports the storage of multidimensional data to save detailed experimental information. Digital imaging and communications in medicine is a set of standards widely used in medical imaging, supporting multilevel and multispectral data storage, ensuring compatibility between different devices and systems and promoting the application of digital pathology.

2.3. Image viewing and analysis platform

A WSI with lossy compression may reach several gigabytes. When the image is decompressed from the file for display and processing, the amount of uncompressed data brings huge challenges to common image-browsing software and computer hardware. When observing histopathology images, the microscope's field of view is adjustable. This requirement allows the image viewing software to dynamically adjust the field of view that needs to be loaded into memory at the moment, obtaining a smooth image browsing experience. Open-source software, such as QuPath,[13] Fiji,[14] CellProfiler,[15] and Icy,[16] provides comprehensive image analysis and user-friendly interfaces. 3D Slicer, a well-known open-source software platform in the field of radiological imaging, also has image viewing and analysis modules for WSI.[17] Furthermore, AI-based pathology toolkits, such as PathML[18] and TIAToolbox,[19] provide researchers with high-performance tools, further promoting the research and application of digital pathology.

3. Digital pathology image analysis

3.1. Stain color normalization

As discussed in Section 2.1, the appearance of WSI varies depending on the parameters used for specimen preparation, such as staining protocols, scanner types, and imaging settings. Stain color normalization aims to reduce or eliminate such differences.

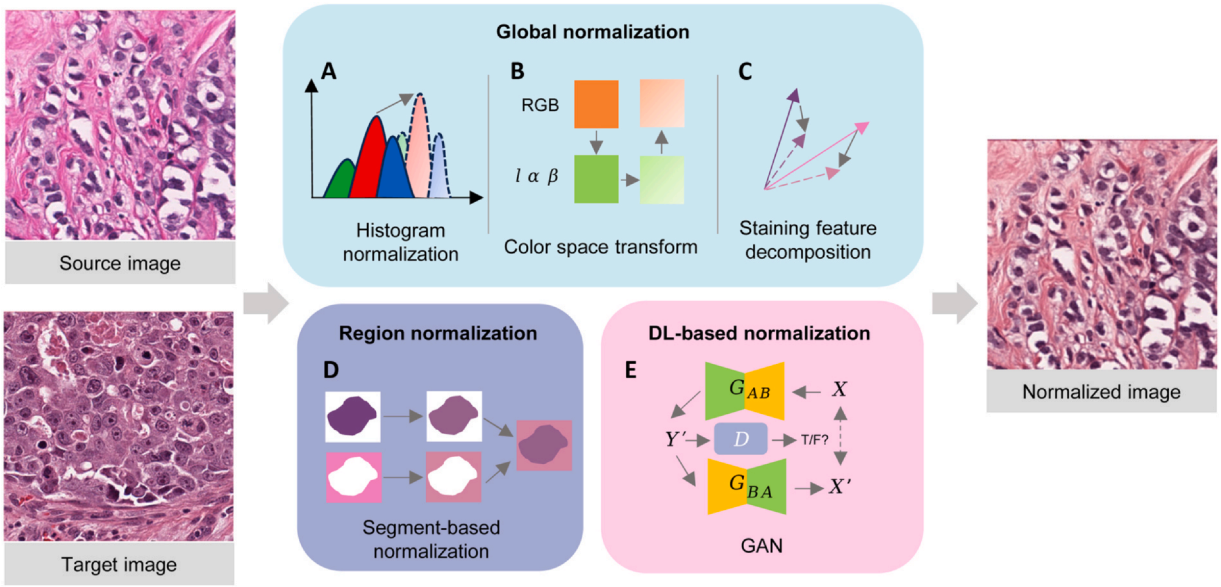


Figure 2. Stain normalization in computational pathology. First, the target image and source image need to be determined. Figure 2A shows the methods based on histogram, Figure 2B shows the methods based on color space, Figure 2C shows the methods based on staining feature decomposition, Figure 2D shows the methods based on region normalization and E shows the methods based on deep learning. (X and X' represent the input data and the reconstructed data, respectively; Y' is the transferred image; G_{AB} and G_{BA} denote the generators that translate images from domain A to B and from domain B to A, respectively). Abbreviations: 1. DL: deep learning 2. GAN: generative adversarial network 3. T/F: true or false 4. D: discriminator.

Techniques for color normalization include color transfer based on the histogram, color space conversion, staining feature extraction, and deep learning (Figure 2). The evaluation of stain normalization can be divided into structure similarity (e.g., multiscale structural similarity index, Pearson correlation coefficient, and root mean square error)[20] and stain separation (e.g., distance-weighted discrimination for measuring staining feature decomposition[21]).

The histogram-based method aligns the histogram distribution of the source image and the target image,[22] although it may ignore the local structure and contrast information, resulting in a loss of details. The color space conversion method proposed by Reinhard et al.[23] converts the image from RGB to other color space for normalization. The images are then transformed back to RGB space. In contrast, staining feature extraction aims to normalize stain information in feature space. The Beer–Lambert law transforms the color space into an optical density space, where image staining information is decomposed into a color appearance matrix and a staining concentration matrix. To better decompose these matrices, several methods are applied, such as empirical prior,[24] singular value decomposition,[21] independent component analysis,[25] non-negative matrix factorization,[26–28] and optimization.[29] However, these methods are often performed globally and do not fully consider the image's local information. Various studies have proposed the use of unsupervised algorithms for pixel classification to achieve region-based normalization, such as K-means, expectation-maximization clustering, and variational Bayesian clustering.[30]

Deep learning techniques also shed light on the color normalization tasks.[31] For example, generative adversarial networks (GANs) have been widely adopted.[20,32–34] Different from the method that relies on a single target image, GAN learns the distribution of the target domain and realizes color style transfer through a deep learning algorithm while maintaining high-resolution information, thereby improving the performance of color normalization. Although the color normalization method based on deep learning can produce high-quality normalized images, the predicted images may affect the performance of the pretrained models and the reliability of generated cases.[35]

3.2. WSI quality control

Artifacts arising from various stages of preparation, scanning, and processing notably degrade the image quality of WSIs. During section preparation, air bubbles and tissue folds are common issues, while uneven section thickness and unstable scanning systems lead to blurriness. Markers, ink traces, dust, and other residues from slide preparation can interfere with image quality, affecting subsequent analysis and interpretation. In clinical practice, standardized procedures are crucial for minimizing artifacts, encompassing standard section preparation, consistent scanning protocols, and robust quality control measures.[36] Quality control (QC) relies on human observation that varies. Computer-aided QC can develop more quantitative methods. QC can be divided into reference-based methods and non-reference-based methods. Reference-based methods compare images with high-quality references to calculate the differences. Non-reference-based methods assess image quality without reference images, offering more adaptability than reference-based QC.

Non-reference-based QC is broadly categorized into traditional feature-based methods and deep learning-based approaches. Feature-based methods use general quality assessment (e.g., color saturation and contrast),[37] novel quality assessment,[38–40] and image features (e.g., texture features,[41] color histograms[42]) combined with classifiers[43,44] to identify common artifacts, such as out-of-focus regions and tissue folds. However, the co-occurrence of multiple artifacts within localized regions further complicates accurate detection and analysis and makes region-level or pixel-level calculation necessary. Using labeled datasets, deep learning models can adapt to multi-artifact prediction and high performance in various scenarios.[45,46] However, their performances heavily depends on the availability of annotated datasets and extensive computation.

Some researchers promoted various toolkits to help pathologists build quantitative and accurate QC. HistoQC combined various feature-based methods to provide a scalable and automated pipeline to quantify artifacts in WSIs.[47] GrandQC provided a pretrained model to detect tissue and artifacts in H&E-stained WSI, driven by large annotated datasets of multiple centers and organs.[48]

3.3. Segmentation in the WSI

Image segmentation extracts various regions of interest (ROIs), such as the nucleus, glands, and tumors. It is the basis for the subsequent quantitative analysis. In what follows, the segmentation is divided into two categories: traditional approaches and deep learning approaches.

3.3.1. Traditional approaches to nucleus segmentation

Because of the distinct color of the nuclei in H&E staining, early studies heavily utilized threshold-based segmentation, which sets a threshold in some appropriate color space.[49,50] Subsequently, the most challenging problem in nucleus segmentation is the "clump" of nuclei. In some scenarios, different types of cells, such as columnar epithelial cells and tumor cells, are found near each other. When the cytoplasm between adjacent cells is not abundant, it appears in the imagery that the nuclei are adhered together. In such cases, traditional threshold-based segmentation methods often result in a clump that includes multiple nuclei. Consequently, the challenge lies in how to separate this clump into individual nuclei, which is a common issue encountered when using conventional methods to segment nuclei. To address this issue, researchers have proposed various methods, such as texture feature clustering,[51–54] the watershed algorithm,[55–58] the graph cut method,[59–61] and active contour.[62,63] However, the performances of these methods are still limited when dealing with complex situations.

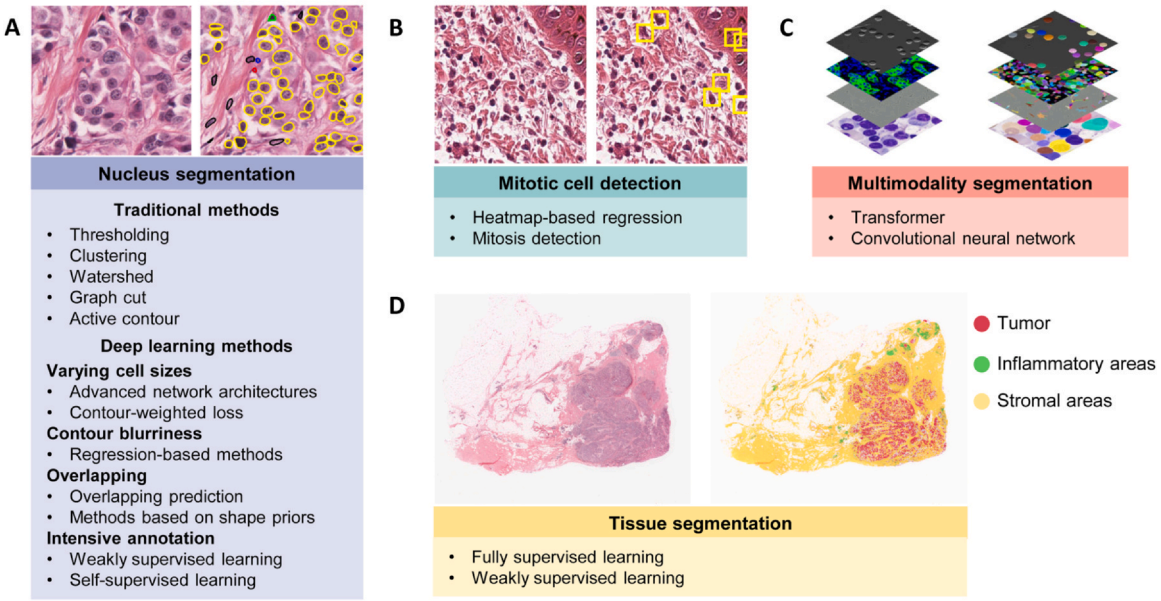


Figure 3. Segmentation in computational pathology. Figure 3A shows nucleus segmentation. Figure 3B shows mitotic cell detection.[79] Figure 3C shows multimodality segmentation. Figure 3D exemplifies tissue segmentation with three types: tumor regions, inflammatory areas, and stromal areas. In Figure 3A–D, the images on the left display the original pathology slides, while the images on the right show the corresponding segmented results. The images of Figure 3A and Figure 3D are annotated by TIAToolbox.[19] The images of Figure 3C are reproduced with permission from the Springer Nature.[80]

3.3.2. Deep learning for segmentation at the cell level

Deep learning methods leverage their feature-learning capabilities to extract boundary features suited to various challenges (Figure 3A), such as varying cell sizes, blurred contours, diverse morphology, and overlapping instances. To address varying cell sizes, numerous studies have focused on improving network architectures and introducing boundary-aware loss functions to enhance multiscale features and boundary feature learning.[64,65] For blurred contours and diverse morphologies, learning detailed boundary information is crucial. Regression-based methods have been employed to predict rich boundary information. These methods predict different types of morphological and boundary details, such as contour masks[66,67] and the spatial distribution of cells.[68–73] Overlapping instances often result from the preparation process and cellular arrangement. Some studies focused on predicting overlapping and nonoverlapping regions.[74,75] Moreover, other researchers proposed leveraging the visible parts of the cell to predict the morphology of occluded instances.[76–78]

Mitotic figures, being a special stage of cells, are closely related to cancer staging and differential diagnosis(Figure 3B). Research has also explored the detection of mitotic figures.[81–83] Due to the varied morphologies and small size of mitotic cells, morphology and contour-based methods alone cannot effectively identify them. Therefore, methods based on object detection[84–86] are widely used in mitotic cell recognition.

Furthermore, reliance on extensive manual annotation and high computational costs present daunting challenges for the development of cell segmentation models. To mitigate the dependency on detailed annotations, weakly supervised learning[87–91] and self-supervised learning[92–98] have emerged as promising alternatives. Additionally, the high resolution of pathology images demands substantial computational resources, which has spurred research on designing lightweight architectures for efficient instance segmentation.[99,100] In addition, the diversity of pathological images, which is influenced by variations in staining techniques and microscopy modalities, further complicates cell segmentation (Figure 3C). As data and model parameters grow, developing a universal cell segmentation model becomes a promising direction.[101] Ma et al.[80] have already built large-scale multimodality datasets for generalizable segmentation models with excellent performance.

3.3.3. Deep learning for segmentation at the tissue level

The composition and distribution of tissues play an important role in the diagnosis and prognosis of cancer. Abundant studies focus on automatically segmenting various tissue types, for instance, tumors,[102,103] glands,[104–106] blood vessels,[107,108] and even multiple tissue types,[109–111] as illustrated in Figure 3D. Owing to the difficulty of pixel-level annotation, some researchers have developed methods based on weakly supervised learning. In weakly supervised learning, the annotation of tissues is sparse, typically consisting of the contours or image-level labels of ROIs. To enrich the label, Xu et al.[112] applied multiple-instance learning techniques to generate instance-level labels for segmentation model training. Chan et al.[113] used a pretrained instance-level tissue classification model to predict pixel-level activation maps, which obtained information on different tissues and served as a pixel-level supervision signal. Zhong et al.[114] used a lightweight model to predict the ROIs and generated pseudo labels through consistency constraints for student network supervision to achieve tissue segmentation.

3.4. Classification in the WSI

The classification of tissue types plays a major role in pathology. Tasks such as differentiating between benign and malignant tumors and measuring lesion areas can benefit from quantitative computation analysis.

3.4.1. Classification with traditional methods

Before the deep learning era, most machine learning methods often relied on pathologists' handcrafted features and used machine learning-based classifiers (e.g., support vector machines [SVMs]) to perform the analysis.[115–117] Nguyen et al.[118] extracted nuclei shape features and textural features using Gabor filters to predict nuclei classification using an SVM classifier in prostate cancer. Basavanhally et al.[119] used nucleus detection by combining region growing and Markov random fields. The detected nuclei were represented as a graph, converted into a graph vector, and input into an SVM classifier to predict lymphocytic infiltration grading in breast cancer. Huang et al.[120] proposed a nuclei segmentation method that combines marker-controlled watershed transform and the active contour technique. They extracted six types of cellular features: nucleocytoplasmic ratio, nuclear irregularity, hyperchromatism, mean nuclear size, anisonucleosis, and nuclear texture. These features were fed into an SVM-based classifier to predict the grading of hepatocellular carcinoma. However, traditional methods suffer from reliance on handcrafted features, which are insufficient for capturing the complex patterns and subtle variations in pathology images.

3.4.2. Classification with deep learning methods

Since their debut, convolutional neural networks (CNNs) have become a mainstream method due to their excellence in image classification.[121,122] Although CNNs have excellent classification capabilities for images of typical small sizes. However, the large sizes of WSIs, which may contain thousands of small images (patches), often make them too big to fit into GPU memory. Integrating CNNs to handle the classification of patches while maintaining superior performance presents a challenge. What makes the situation more challenging is the heterogeneity among these patches. Hou et al.[123] proposed a method based on fusing local CNN classification and overall WSI statistics. Many subsequent studies on WSI classification have drawn inspiration from this approach.[124–126]

However, there is a bottleneck in improving WSI classification performance due to the expensive cost of outlining pathology data, particularly for large WSIs. Fortunately, multiple instance learning (MIL) provides new insights for pathology image classification. MIL excels in tissue classification due to its ability to handle uncertain labels and complex scenarios. Given the high resolution of WSIs and the cost of pixel-level annotation, MIL splits WSIs into instances and treats a set of instances as a bag, leveraging both local and global image information for efficient classification using bag-level labels. This approach minimizes reliance on pixel-level or instance-level labels, addressing the challenges of processing super high-resolution images and sparse labeling.

MIL's effectiveness in pathology image analysis hinges on three components: instance feature extraction, aggregation, and classification. For feature extraction, pretrained CNNs[127] and self-supervised extractors[128,129] are utilized. In terms of feature aggregation, traditional methods (for instance, mean and maximum aggregation[130,131]) can be hindered by noisy instances. Attention mechanisms[128,132,133] and transformer networks,[134] as shown in Figure 4A and 4B, boost the aggregation ability by weighting instance features and capturing instance-to-instance contextual information, respectively. Attention-based feature aggregation is used to predict the attention scores of patch features and sum the patch features with attention weights. In contrast, transformer-based feature aggregation involves inputting a class token and patch features added with positional embeddings into a transformer network for feature aggregation, and finally using the output class token as the WSI feature. Additionally, graph neural networks offer a sophisticated approach to feature aggregation by capturing complex node and edge relationships.[135] Different from the previous two methods of feature aggregation, graph neural networks can adapt to various feature types[136–139] and integrate multiscale features,[140–142] as illustrated in Figure 4C.

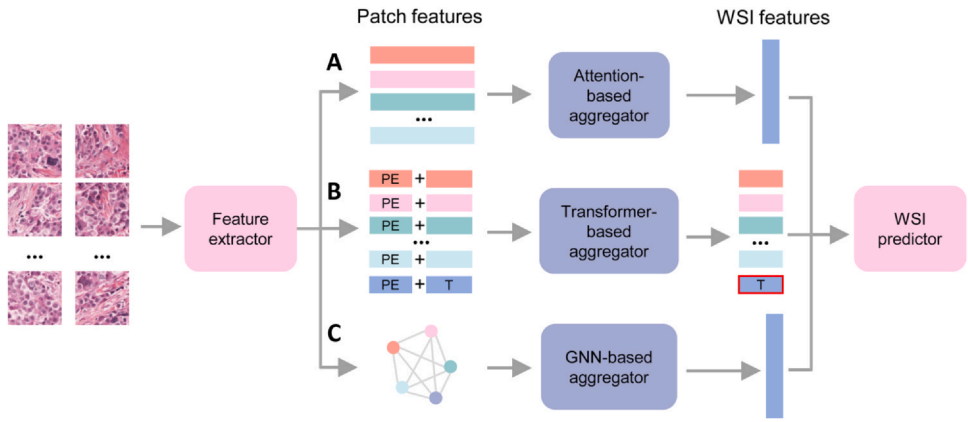


Figure 4. Multiple instance learning in computational pathology. Multiple instance learning computes the patch features from the patches using a feature extractor and inputs the final whole-slide image (WSI) features into a WSI-based classifier for prediction after different feature aggregation methods. Multiple instance learning has different feature aggregation methods. Figure 4A displays attention-based feature aggregation, Figure 4B displays transformer-based feature aggregation, including position embeddings (PEs) and a class token (T), and Figure 4C displays feature aggregation based on graph neural networks (GNNs).

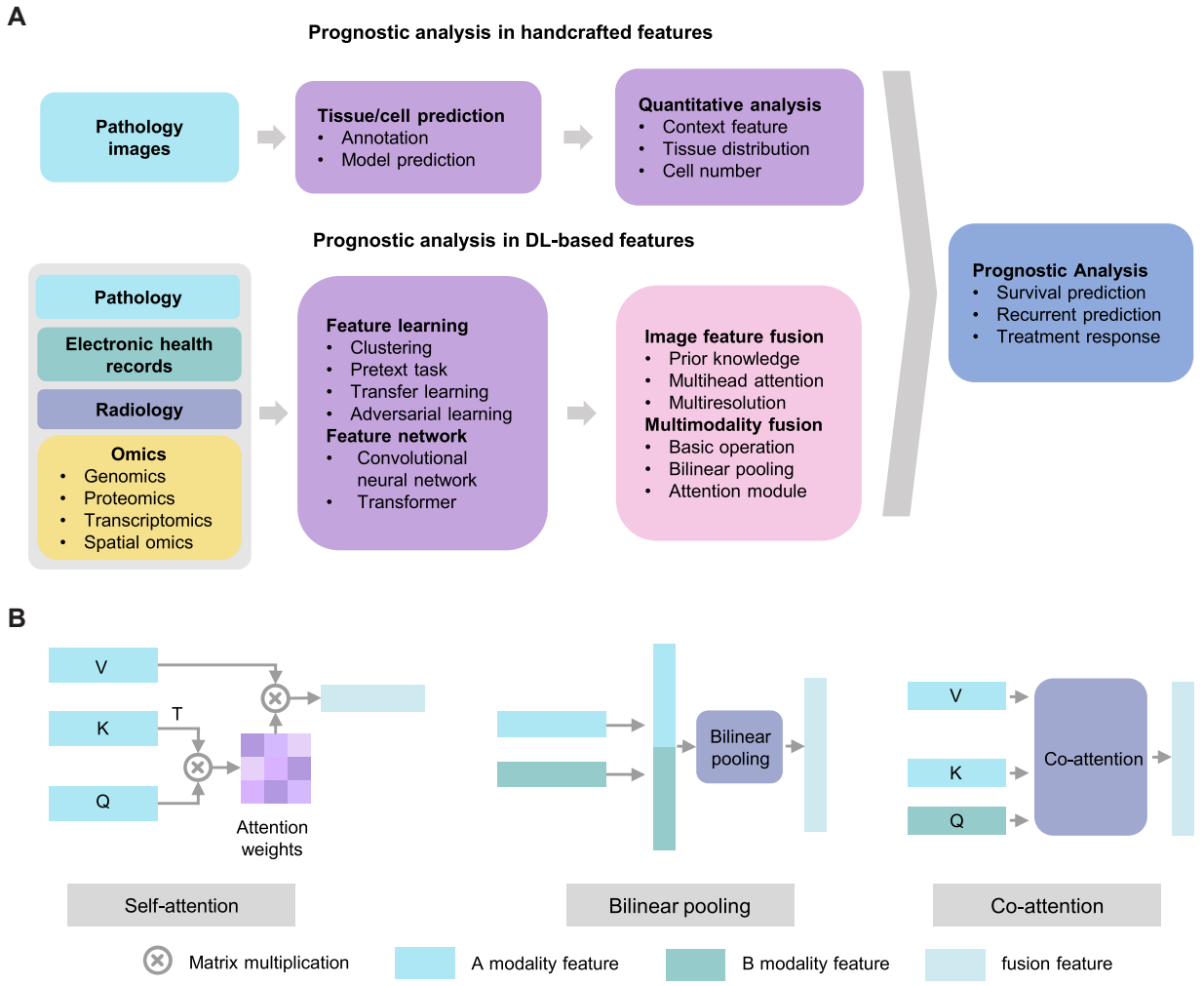


Figure 5. Prognostic analysis in computational pathology. Figure 5A illustrates prognosis analysis in computational pathology. Figure 5B illustrates fusion modules. Abbreviations: 1. V: Vector 2. K: Key 3. Q: Query 4. T: Transpose.

3.5. Prognostic analysis with computational pathology

Prognostic analysis predicts disease progression and outcomes, offering critical insights for doctors to enhance treatment strategies and patient survival rates. In computational pathology, prognostic analysis enables the precise capture of microenvironmental features in pathology images, aiding in disease progression prediction. It uncovers patterns that are difficult for pathologists to identify through visual inspection, improving prognostic accuracy. This section will cover two prognostic analysis methods: handcrafted feature-based and deep learning-based approaches (Figure 5).

3.5.1. Prognostic analysis based on handcrafted features

The prognosis assessment of tumors is inseparable from factors such as the local microenvironment of the lesion and global structural traits. These factors serve as biomarkers to manifest the information, which mainly requires manual annotation or model prediction to acquire ROIs and calculate the quantitative features of ROIs, including tumor matrix cell ratio, immune infiltration abundance, tissue cell number, tissue texture features, and cell nuclear morphology features.[143–147] The calculated features are then used for prognostic analysis.

In model prediction, studies have shown that H&E staining images can predict prognostic factors, namely biomarkers, manifesting gene mutations, gene expression, and microsatellite instability.[148,149] Biomarkers are typically detected using expensive and time-intensive techniques, such as IHC staining and fluorescence *in situ* hybridization. Therefore, much research focuses on predicting biomarkers based on conventional H&E staining, providing economical and efficient detection and prognostic analysis. Numerous studies have been conducted on bladder cancer,[150] colorectal cancer,[151] breast cancer,[127,152,153] uveal melanoma,[154] and ovarian cancer.[155] Microsatellite instability is an indispensable factor in the prognosis of gastrointestinal cancer, and studies have shown the effectiveness of predicting microsatellite instability using H&E staining images.[151,156,157]

3.5.2. Prognostic analysis based on deep learning features

Due to the complexity and diversity of diseases, the limited handcrafted features may not be sufficient for the prognosis, especially when combined with more modalities. In addition, with the increasing number of treatment types, the "right-hand side" of prognosis prediction becomes progressively more complex, leading to further increases in diagnosis and treatment costs. Therefore, studies have proposed AI-based methods to mine biomarkers with good prognostic stratification characteristics in pathology images, which helps improve the accuracy of treatment decisions and the efficiency of studying the pathological mechanisms of the disease. In this section, we will introduce the prognostic analysis based on pathology images and multimodality data (Figure 5A).

Prognostic analysis based on pathology images. Here, the deep learning algorithm first extracts the features from the image at multiple scales as well as at multiple locations and then builds a predictive model for prognosis prediction. Multiple studies use clustering,[158] pretext task,[159,160] transfer learning,[161,162] and adversarial generative learning,[163] among other strategies, to alleviate the problem of low performance of deep learning survival analysis caused by a small number of datasets. For the feature interaction learning in survival analysis, a variety of improved methods are used to optimize performance, such as ranking-based methods,[164] multihead attention,[165] and multiresolution learning.[166] To improve interpretability, several researchers have proposed interpretability modules to identify important patches and unique morphological-physiological attributes[167] and have combined attribution algorithms to locate and mine biomarkers.[168]

Prognostic analysis based on multimodality data. Although many studies concentrate on single-modality survival prediction, there are limitations to relying solely on the modality of pathology images. Clinically, survival analysis requires multimodality information, including radiology images, pathology images, clinical information, and genetic information, each of which contributes distinct insights into the patient's condition. Integrating different modalities helps discover new biomarkers and promote personalized medicine. In multimodality learning, the fusion of different modalities gives rise to complex relationships, and modeling complex multimodality interaction features is critical. Early studies used operations such as feature concatenation, maximum fusion, mean fusion, and bit-wise addition to perform feature fusion.[169–172] However, there are certain complex correlations between different multimodality features, and simple concatenation may not be able to capture the deep relationships between modalities. Several studies have proposed fusion modules based on Kronecker products and gating attention to mine the relationship between modalities to enhance the feature representation across multiple modalities.[173–175] Additionally, some strategies are used for multimodality feature fusion, such as bilinear pooling,[176–178] and co-attention module,[179–181] as illustrated in Figure 5B. Bilinear pooling extracts interactive features between modalities, but redundant features limit model improvement. Co-attention enhances feature mining by calculating independent vectors and generating interpretable attention maps. Furthermore, some advanced attention mechanisms are emerging in multimodality learning, such as the fusion of pathology images and transcriptomics data based on transformers[182] and the fusion of pathology images and genetic data based on self-attention and cross-attention.[183]

3.6. Foundation models in computational pathology

Foundation models are pretrained large-scale models used for various downstream tasks across domains.[184–187] With the rise of self-supervised learning, powerful foundation models can now be built by leveraging large, unlabeled datasets, enabling better feature learning and generalization.

3.6.1. Model scale

It is well known that it is difficult to collect large-scale medical datasets due to the frequency of image acquisition and the challenges of data sharing. At present, foundation models mainly rely on public and private datasets (Figure 6A). The Cancer Genome Atlas, a public dataset, contains approximately 29,000 WSIs, covering 32 cancer types.[3] Private datasets are usually larger, such as the approximately 1.5 million WSIs collected by the Memorial Sloan Kettering Cancer Center ,[188] the roughly 420,000 WSIs collected by the Mount Sinai Health System,[189] and the nearly 100,000 WSIs from the collaboration between three institutions.[190] Additionally, Dippel et al.[191] proposed the foundation model RudoIfV, trained on the 133,998 WSIs covering diverse preprocessing protocols and data sources across regions. Xu et al.[192] introduced a foundation model called Prov-GigaPath, which was trained on 171,189 WSIs from 28 cancer centers. With the expansion of pathology data, the number of modalities is also increasing, such as multistain data.[191,193] Image–text-based models are also constantly evolving, such as OpenPath,[194] Quilt-1M,[195] and the 1.17 million pathology image–text pairs from the public used to train the visual-language foundation model, Contrastive learning from Captions for Histopathology,[196] as illustrated in Figure 6B and 6C.

CNNs and visual transformers (ViTs) are the main backbone architectures of foundation models.[197] CNN uses local convolution kernels for feature extraction with translation invariance, while ViT leverages self-attention for global information and has a larger receptive field. At present, the network parameters of the mainstream CNNs (e.g., ResNet) and ViTs are 12–60 M and 86–632 M, respectively. ViT has more parameters than CNN, enabling better adaptation to large-scale data. Combined with self-supervised learning, ViT performs well in extracting more general representation and has been widely used in the backbone network of foundation models.[188–196,198] Moreover, the transformer architecture shows its outstanding performance in tasks across multiple modalities, demonstrating its potential in the multimodality field.[185]

3.6.2. Self-supervised learning

Unlike traditional supervised learning, self-supervised learning uses the characteristics of the data itself to learn a representation of data, without the need to manually label a large amount of data. This characteristic can effectively deal with the problems of large scale and the difficult labeling of pathology images, rendering self-supervised learning widely adaptable in the field of pathology.

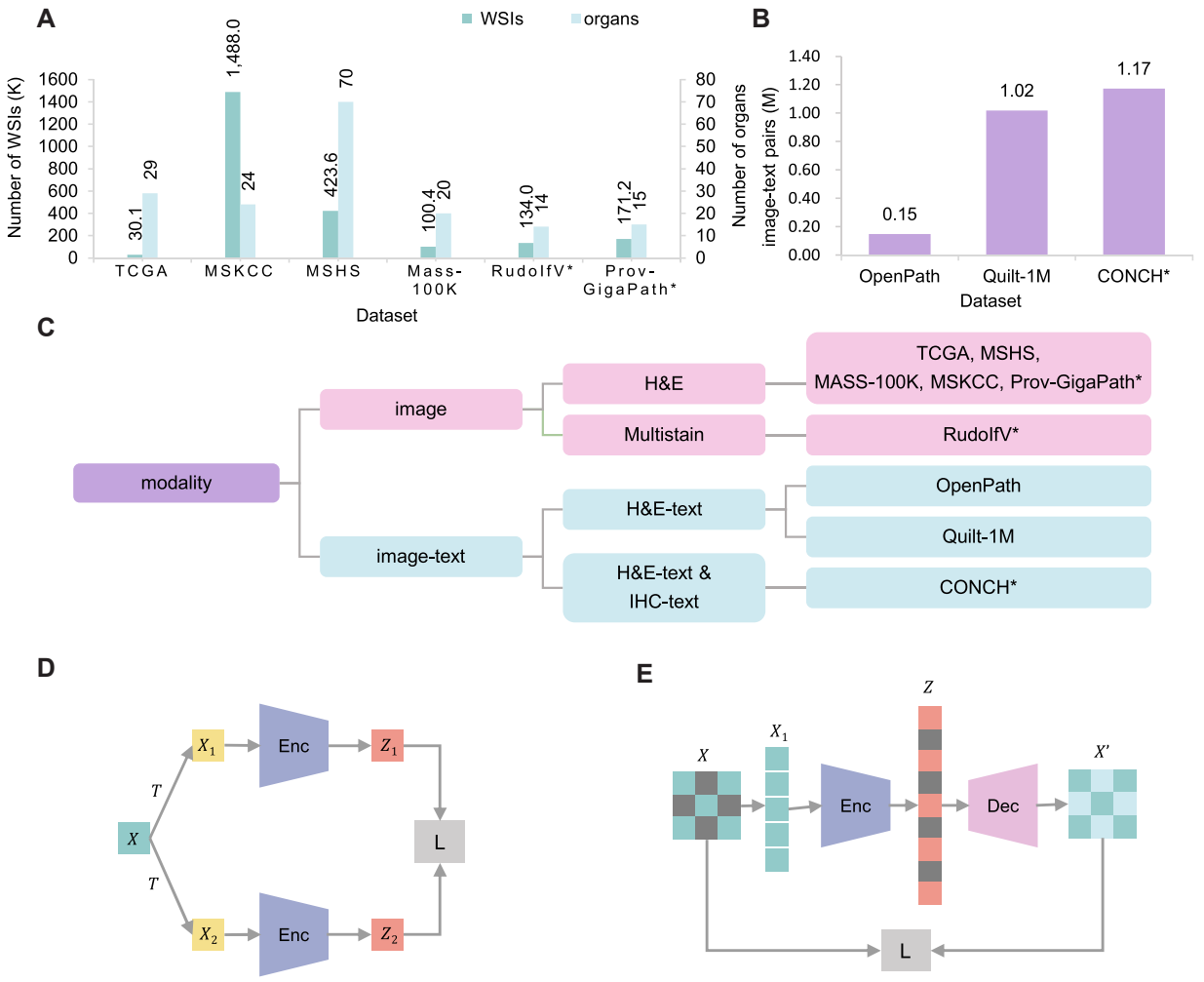


Figure 6. Data scale in computational pathology. Figure 6A is the comparison of large-scale pathology image datasets by the number of WSIs and organs, Figure 6B is the comparison of multimodality datasets by the number of image–text pairs, and Figure 6C is the illustration of the modality of large-scale datasets. Figure 6D is a framework of contrastive learning. Figure 6E is a framework of generative learning. X and X' represent the input and reconstructed data, respectively. X_1 and X_2 are the augmented data generated by transformation T. Z_1 and Z_2 denote the features of X_1 and X_2, respectively. Z denotes the features computed by the model from the input X. * represents the name of the model trained on this dataset. Abbreviations: 1. MSKCC: Memorial Sloan-Kettering Cancer Center 2. MSHS: Mount Sinai Health System 3. TCGA: The Cancer Genome Atlas 4. L: loss function 5. Enc: encoder 6. Dec: decoder 7. CONCH: contrastive learning from captions for histopathology.

The algorithms of self-supervised learning and their applications in foundation pathology models can mainly be divided into the following categories: contrastive learning, generative learning, and hybrid methods (Figure 6d and 6e). Contrastive learning is an important method of self-supervised learning. By minimizing the loss function of positive and negative samples, the feature representation learned by the model allows for closer similar samples and farther dissimilar samples, effectively learning sample features, such as momentum contrast,[199] simple framework for contrastive learning of visual representations,[200] and self-distillation with no labels (DINO).[201,202] Pathology foundation models based on contrastive learning have been developed to a certain extent.[193,203–205] Most of the work is mainly based on the DINO series.[188,190–192] Kang et al.[206] compared multiple self-supervised learning methods on a large-scale dataset, and the results showed that the DINO pretrained model outperforms others overall. In addition, contrastive language–image pretraining (CLIP) is based on the image–text contrastive learning algorithm.[185] Multiple studies have constructed foundation models of pathology images and text data based on the CLIP framework.[194,195,207,208] Generative learning is another self-supervised learning method that learns image features by reconstructing images and has achieved remarkable success in natural language processing (e.g., bidirectional encoder representations from transformers[209] and generative pretrained transformers.[186,187]) Luo et al.[210] proposed BioGPT, a large language model tailored for the biomedical domain. In computer vision, the masked autoencoder has highlighted the potential of generative learning[211] and has been subsequently applied in several pathology foundation models.[189,202]

Recent studies have combined contrastive and generative learning to enhance self-supervised learning in ViT (e.g., image bidirectional encoder representations from transformers pretraining with online tokenizer[212]) leveraging its strong performance in computational pathology.[198] In the multimodality foundation model, contrastive captioners extend CLIP networks with a

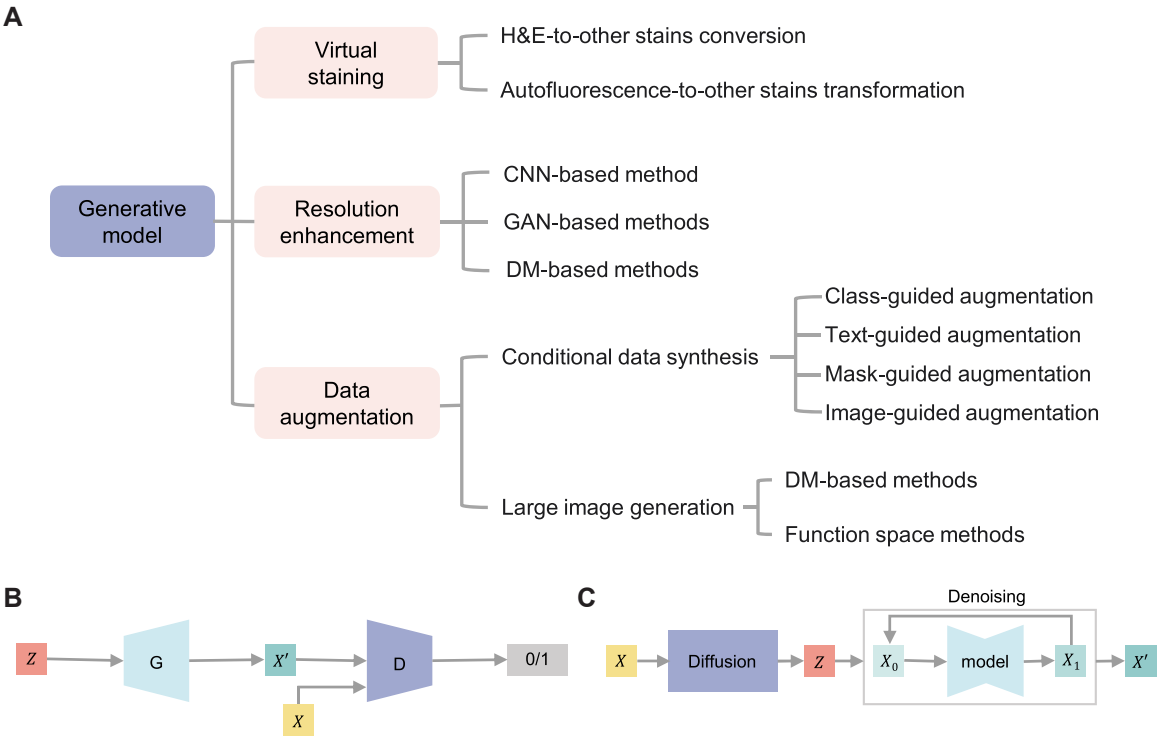


Figure 7. Generative AI (GenAI) methods. Figure 7A consolidates the application of GenAI in pathology images. Figure 7B is a framework of generative adversarial networks (GANs). Figure 7C is a framework of diffusion models (DMs). X and X' represent the input data and the reconstructed data, respectively. X_0 and X_1 represent denoising data in the denoising process of the diffusion model. Z denotes the noisy data. Abbreviations: 1. G: generator 2. D: discriminator.

multimodality text decoder. Contrastive captioners leverages contrastive and generative methods to enhance performance on complex vision-language tasks (e.g., visual question answering),[213] commonly applied in pathology foundation models.[196,214–216]

3.7. Generative models in computational pathology

Generative AI (GenAI) learns data distributions and latent patterns from training data to generate new samples. With rapid advancements in GenAI technology, numerous applications have emerged across fields, including text processing, code optimization, and art creation. In healthcare, GenAI is gradually being applied in areas such as report generation and data augmentation. In this section, we will introduce the algorithms from GenAI and summarize the applications in the field of pathology (Figure 7A).

3.7.1. Algorithms

GenAI has evolved alongside deep learning, with current mainstream algorithms falling into five categories: autoregressive models, GANs, variational autoencoders, flow-based models, and diffusion models. GANs and diffusion models are particularly common in pathological image generation. GANs use adversarial training between generators and discriminators, where generators create realistic fake data to deceive the discriminators, though their training is unstable and prone to failure(Figure 7B). In contrast, diffusion models generate samples by adding noise to data and then denoising it through a reverse process, producing higher-quality images but requiring substantial computational resources (Figure 7C).

GenAI models are evaluated using content-related and content-unrelated metrics. Content-related metrics for images (e.g., inception score[217] and Fréchet inception distance[218]) assess quality and diversity, while text metrics (e.g., bilingual evaluation understudy[219] and recall-oriented understudy for gisting evaluation[220]) evaluate similarity to references. Content-unrelated metrics, such as structural similarity index measure and peak signal-to-noise ratio for images, assess structure similarity and perceptual quality.[221] Additionally, human discrimination by experts is often used for validation.

3.7.2. Virtual staining

In clinical practice, multiple stains are used for accurate diagnosis, but tissue sampling is in high demand, and the pathology analysis process is time-consuming. Multiplexing and advanced imaging techniques can mitigate some of these challenges but are costly. With the rise of GenAI, virtual staining technology has emerged as a promising solution. Virtual staining uses generative algorithms to simulate traditional staining processes, reducing time and operational costs while maintaining diagnostic accuracy.

Virtual staining is mainly transformed by H&E images, which are the most commonly used staining images in clinical practice, and are converted to other special staining (e.g., IHC and PAS) through H&E images. Early algorithms relied on data registration, but

later unpaired style transfer methods minimized the need for paired data, improving algorithm flexibility and data scalability.[222] To enhance the reliability of the data, numerous studies have improved the GenAI network to enhance the feature learning of prior information, such as pathological structure,[223] staining,[224] and tissue mask.[225,226] Dubey et al.[227] proposed a text-guided latent diffusion model combined with an adversarial training module to achieve high-quality virtual staining from H&E to multiplexed IHC. Ghahremani et al.[5] proposed a GAN-based method for transferring IHC images to immunofluorescence images. Pati et al.[228] proposed an AI toolkit that generates multiplexed IHC images from H&E images.

Autofluorescence imaging uses ultraviolet or visible light to excite endogenous fluorophores in tissues or cells, emitting fluorescence that reveals tissue structure and function. It offers critical diagnostic insights without the need for extensive preparation or exogenous dyes.[229] Current research is exploring the use of autofluorescence images for virtual staining, enabling the conversion of these images into conventional staining formats, such as H&E, PAS, Jones' methenamine silver, and Masson's trichrome.[4,6,230–232]

3.7.3. Resolution enhancement

WSIs often suffer from blur and low resolution due to hardware constraints or imaging noise. Moreover, acquiring high-resolution images in clinical settings is often time-consuming and costly. To address this, several studies have developed super-resolution techniques based on CNN variants, leveraging their powerful feature learning capabilities.[233–235] Additionally, GenAI-based algorithms, such as GANs[236,237] and diffusion models,[238] have been explored. However, super-resolution reconstruction faces challenges due to tissue-specific texture differences. Yang et al.[239] proposed a transformer-based model with region attention, using semantic mask information from a large segmentation model for cross-attention calculation, guiding the model to focus on key regions and generate high-quality super-resolution images. Chen et al.[240] introduced a spatiotemporal control algorithm based on reinforcement learning, which does not rely on prior information and uses tile selection and reconstruction time control strategies.

3.7.4. Data augmentation

AI algorithms require diverse data for improved generalization, but the medical field faces challenges due to inconsistent equipment and processes across centers. Additionally, rare diseases are often underrepresented in medical datasets, with data collection processes being time-consuming, expensive, and limited by ethical constraints.

Data augmentation helps improve model generalization by generating new training samples through transformations of original images. Traditional augmentation methods rely on basic color and spatial transformations but fail to capture granular differences crucial for model performance, including color jitter, flip, rotation, and random crop. To further enhance data augmentation, studies show that GenAI algorithms effectively improve downstream classification tasks.[241,242] Several researchers have proposed GenAI models to address the domain shift from acquisition difference[243] and pathological feature transition.[244] Conditional GenAI allows for better control of the generation process. Various studies have proposed information-guided diffusion models (e.g., image feature embedding,[245] class embedding,[246,247] and mask embedding[248]). In cell segmentation, GenAI-based augmentation reduces the burden of annotating fine labels, such as GAN-based methods[91,249–251] and diffusion models.[252–254] However, existing labels are limited, resulting in a lack of sample diversity. Some studies have proposed methods to synthesize both images and labels simultaneously.[255] Additionally, incorporating textual information in certain approaches allows for better control of the diversity and quality of generated segmented data.[256]

While the above methods focus on tile-level data augmentation, generating larger images remains challenging due to the high computational cost and the need for consistent context modeling across the entire image. Diffusion models have emerged as a mainstream solution due to their iterative strategy and flexible guidance mechanism. Many methods use tile-based techniques due to model input size limitations. A number of studies explore tile-feature-guided large image generation,[257] but they suffer from edge inconsistencies from different tiles. To address this, dynamic tile reconstruction strategies have been proposed, such as grid movement[258] and random sampling.[259,260] In contrast, Le et al.[261] introduced a framework that avoids tile reconstruction by using a conditional diffusion model based on function space and attention neural operators, enabling the generation of high-quality super-resolution and large images (up to 4096 × 4096 pixels) using multiple forms of image guidance, such as text and images.

4. Challenges

At present, AI has achieved considerable success in medical imaging, but the clinical implementation of AI is relatively slow. The security of its algorithm and data is an important key factor. AI security spans multiple stages, from data collection and model training to the final application, making it a key consideration in the successful deployment of AI in healthcare.

4.1. Data bias and privacy

Data collection creates a number of data biases, such as disease, racial, gender, and acquisition biases.[262] These biases reflect the data for model inference, and the bias of its predictions can affect the judgment of doctors and users. In model training, some strategies can reduce biases in the model, such as fairness constraints[263] and weighted sampling.[264,265] Data bias can be further reduced by building larger datasets and through regulation by professionals for bias research.[266] Additionally, integrating causal analysis with these approaches facilitates a more effective reduction of bias.[267,268]

The privacy of clinical data presents another challenge. Many countries have enacted policies (for instance, the Health Insurance Portability and Accountability Act in the United States and the General Data Protection Regulation in the European Union)[269] to protect data privacy, making access to clinical data more difficult. To address this, several studies have proposed federated learning

as a solution.[270] Federated learning enables collaborative model training across multiple local centers without the need to centralize data, thereby reducing the risk of data leakage. In the inference phase, privacy-preserving algorithms, including homomorphic encryption, differential privacy, and secure multiparty computation, have also been explored to ensure data security and privacy.[271]

4.2. Model explainability and causality

While AI-based pathology is developing rapidly, the "black box model" poses a huge concern for those in the field of medical research. In terms of interpretability, many studies have proposed a variety of methods to interpret models, mainly through visual interpretability (e.g., prototype,[272,273] gradient-based methods,[274–276] feature disentanglement[277,278] and graph-based methods[279,280]) and attribution explainability (e.g., concept attribution[281,282] shapley values[283–285] and local interpretable model-agnostic explanations[286]).

The lack of causality can undermine the reliability of predictions. Models often capture correlations instead of causal relationships. Causal-based methods focus on causal constraints in model training and counterfactual reasoning for interpretability. Causal constraints mitigate confounding effects using causal graphs or structural equation models to capture feature dependencies.[268,287–289] Additionally, counterfactual reasoning simulates "what would happen if" scenarios, revealing the decision-making process and the impact of features. This method helps data augmentation distribution[290,291] and provides a new perspective of interpretability[292,293] with causal mechanisms.

4.3. Reproducibility

Deep learning model performance and stability are heavily influenced by the training process, data distribution, and hyperparameters. Additionally, program accessibility is crucial for researchers and medical staff. To improve reproducibility and transparency in medical AI, organizations are developing checklists,[294–296] that provide guidelines on data collection, research design, model development, evaluation, and explainability.

4.4. Regulation

The development and deployment of AI-based pathology products require strict regulation owing to their direct impact on medical diagnoses and patient outcomes. Because of their unique nature, their regulation differs from that of other product categories. Over the years, different countries have had varying attitudes toward approval. The Food and Drug Administration has maintained a relatively open attitude toward the medical application of medical AI, allowing AI products to make adaptive improvements[297] in the United States. At present, in the European Union, a more conservative attitude will be maintained and large changes to the model will not be allowed. Risk stratification is detailed for the application of medical AI products, with different approval forms for different risk levels.[298]

5. Outlook

Currently, computational pathology can perform many intelligent diagnostic tasks, including cell segmentation and tumor classification. In addition, computational pathology has shown great potential in the exploration of prognostic information. With advancing technology, the modality of computational pathology has evolved from single-dimensional data to multi-dimensional data, which has brought new challenges. The development of 3D pathology imaging and spatial omics has enabled computational pathology to move closer to the goal of precision medicine.

3D pathology technology has made considerable progress at this stage, which, combined with objective machine learning-based analysis methods, is dedicated to improving the reproducibility and reliability of diagnosis.[299] 3D pathology can effectively characterize and quantify spatial relationships between cells, which is especially suitable for analyzing the tumor immune microenvironment; for example, the interaction between programmed death-1 and programmed death-ligand 1[300] can identify rare key cells (for instance, tumor progenitor cells[301] and cancer stem cells[302]) that are difficult to detect with traditional thin sections. Combined with computational pathology algorithms, it helps to understand tumor heterogeneity, promoting cancer research and treatment strategies.[303] Currently, imaging techniques that are widely used in 3D pathology include optical clearing, confocal microscopy, multiphoton microscopy, and light sheet microscopy.[304] Various novel imaging technologies provide pathologists with deeper information on tissue structure and cell distribution. The future development of 3D pathology will rely on technological innovation, interdisciplinary collaboration, regulatory support, and broad acceptance by the medical community.

In recent years, spatial omics analysis has become an active topic. It displays transcriptomics, proteomics, and metabolomics in tissue space, providing more detailed microenvironment information.[305] However, the acquisition and processing of spatial omics information are full of challenges under high-throughput data.[306] The cost of spatial omics is relatively high; consequently, spatial omics have not yet been widely used in clinical practice. Various studies have shown that microenvironment information can be predicted through widely used H&E images. Therefore, it is of great significance to use spatial omics information to make predictions concerning common H&E images.[307] This method can further expand the application range of H&E images, alleviating the need for complex staining.

Moreover, with the continuous development of deep learning technology, building a foundation model has become an important task.[101,196,308] Currently, pathology image datasets based on multiple modalities are increasing rapidly, providing rich data resources

for training more powerful models.[80] In the future, developing models that adapt to multimodality image analysis may become a major trend.

6. Conclusions

Computational pathology has unleashed its enormous potential from clinical diagnosis to medical research. Driven by AI, automatic pathology analysis improves the efficiency of routine clinical workflow and boosts the exploration of comprehensive medical research. In the future, more advanced technologies, such as 3D pathology and spatial omics, will enrich the diversity of pathology interpretations. With the proliferation of AI, computational pathology is evolving to achieve greater generalization and precision.

CRediT authorship contribution statement

Qinqin Huang: Writing – original draft, Visualization, Investigation, Writing – review & editing. **Shen'ao Wu:** Writing – original draft, Investigation. **Zhenkai Ou:** Writing – original draft, Investigation. **Yi Gao:** Writing – review & editing, Supervision.

Declaration of Competing Interest

The authors declare that they have no known competing financial interests or personal relationships that could have appeared to influence the work reported in this paper.

Acknowledgments

This work was supported in part by the Shenzhen Natural Science Fund (the Stable Support Plan Program 20220810144949003), the Key Technology Development Program of Shenzhen (JSGG20210713091811036), the Key-Area Research and Development Program of Guangdong Province (2021B0101420005), the Shenzhen Key Laboratory Foundation (ZDSYS20200811143757022) and the Guangdong Provincial Key Laboratory of Mathematical and Neural Dynamical Systems (2024B1212010004).

References

1. Malon CD, Cosatto E. Classification of mitotic figures with convolutional neural networks and seeded Blob features. *J Pathol Inf.* 2013;4(1):9.
2. Cruz-Roa A, Basavanhally A, González F, et al. Automatic detection of invasive ductal carcinoma in whole slide images with convolutional neural networks. *Medical Imaging 2014: Digital Pathology.* SPIE; 2014:904103.
3. Tomczak K, Czerwińska P, Wiznerowicz M. The cancer genome atlas (TCGA): an immeasurable source of knowledge. *Współczesna Onkol.* 2015;19(1A):A68–A77.
4. Rivenson Y, Wang H, Wei Z, et al. Virtual histological staining of unlabelled tissue-autofluorescence images via deep learning. *Nat Biomed Eng.* 2019;3(6):466–477.
5. Ghahremani P, Li Y, Kaufman A, et al. Deep learning-inferred multiplex immunofluorescence for immunohistochemical image quantification. *Nat Mach Intell.* 2022;4(4):401–412.
6. Yang X, Bai B, Zhang Y, et al. Virtual stain transfer in histology via cascaded deep neural networks. *ACS Photonics.* 2022;9(9):3134–3143.
7. Liu S, Hoess P, Ries J. Super-resolution microscopy for structural cell biology. *Annu Rev Biophys.* 2022;51:301–326.
8. Ma L, Luo K, Liu Z, Ji M. Stain-free histopathology with stimulated raman scattering microscopy. *Anal Chem.* 2024;96(20):7907–7925.
9. Taylor MJ, Lukowski JK, Anderton CR. Spatially resolved mass spectrometry at the single cell: recent innovations in proteomics and metabolomics. *J Am Soc Mass Spectrom.* 2021;32(4):872–894.
10. Mohammadi FS, Mohammadi SE, MojaradAdi P, Mirkarimi SMA, Shabani H. A comparative analysis of pairwise image stitching techniques for microscopy images. *Sci Rep.* 2024;14(1):9215.
11. Goldberg IG, Allan C, Burel JM, et al. The open microscopy environment (OME) data model and XML file: open tools for informatics and quantitative analysis in biological imaging. *Genome Biol.* 2005;6(5):R47.
12. Clunie DA. DICOM format and protocol standardization–a core requirement for digital pathology success. *Toxicol Pathol.* 2021;49(4):738–749.
13. Bankhead P, Loughrey MB, Fernández JA, et al. QuPath: open source software for digital pathology image analysis. *Sci Rep.* 2017;7(1):16878.
14. Schindelin J, Arganda-Carreras I, Frise E, et al. Fiji: an open-source platform for biological-image analysis. *Nat Methods.* 2012;9(7):676–682.
15. Lamprecht MR, Sabatini DM, Carpenter AE. CellProfiler™: free, versatile software for automated biological image analysis. *BioTechniques.* 2007;42(1):71–75.
16. De Chaumont F, Dallongeville S, Chenouard N, et al. Icy: an open bioimage informatics platform for extended reproducible research. *Nat Methods.* 2012;9(7):690–696.
17. Yu X, Zhao B, Huang H, et al. An open source platform for computational histopathology. *IEEE Access.* 2021;9:73651–73661.
18. Rosenthal J, Carelli R, Omar M, et al. Building tools for machine learning and artificial intelligence in cancer research: best practices and a case study with the PathML toolkit for computational pathology. *Mol Cancer Res.* 2022;20(2):202–206.
19. Pocock J, Graham S, Vu QD, et al. TIAToolbox as an end-to-end library for advanced tissue image analytics. *Commun Med.* 2022;2(1):120.
20. Salehi P, Chalechale A. Pix2Pix-based stain-to-stain translation: A solution for robust stain normalization in histopathology images analysis. In: 2020 International Conference on Machine Vision and Image Processing (MVIP). IEEE; 2020:1-7.
21. Macenko M, Niethammer M, Marron JS, et al. A method for normalizing histology slides for quantitative analysis. *2009 IEEE International Symposium on Biomedical Imaging: From Nano to Macro.* IEEE; 2009:1107–1110.
22. Tam A, Barker J, Rubin D. A method for normalizing pathology images to improve feature extraction for quantitative pathology. *Med Phys.* 2016;43(1):528–537.
23. Reinhard E, Adhikhmin M, Gooch B, Shirley P. Color transfer between images. *IEEE Comput Graph Appl.* 2001;21(4):34–41.
24. Ruifrok AC, Johnston DA. Quantification of histochemical staining by color deconvolution. *Anal Quant Cytol Histol.* 2001;23(4):291–299.
25. Alsubaie N, Trahearn N, Raza SEA, Snead D, Rajpoot NM. Stain deconvolution using statistical analysis of multi-resolution stain colour representation. *PLoS One.* 2017;12(1):e0169875.
26. Bilgin C, Rittscher R, Filkins R, Can A. Digitally adjusting chromogenic dye proportions in brightfield microscopy images. *J Microsc.* 2012;245(3):319–330.
27. Vahadane A, Peng T, Sethi A, et al. Structure-preserving color normalization and sparse stain separation for histological images. *IEEE Trans Med Imag.* 2016;35(8):1962–1971.
28. Li X, Plataniotis KN. A Complete color normalization approach to histopathology images using color cues computed from saturation-weighted statistics. *IEEE Trans Bio-Med Eng.* 2015;62(7):1862–1873.
29. Zhou N, Gao Y. Optimized color decomposition of localized whole slide images and convolutional neural network for intermediate prostate cancer classification. *Proc SPIE.* 2017;10140:101400W.

30. Hoffman RA, Kothari S, Wang MD. Comparison of normalization algorithms for cross-batch color segmentation of histopathological images. In: *2014 36th Annual International Conference of the IEEE Engineering in Medicine and Biology Society*. IEEE; 2014:194-197.
31. Bug D, Schneider S, Grote A, et al. Context-based normalization of histological stains using deep convolutional features. international workshop on deep learning in. *Med Image Anal.* 2017;10553:135–142.
32. Cho H, Lim S, Choi G, Min H. Neural stain-style transfer learning using GAN for histopathological images. *arXiv preprint arXiv:171008543*. Published online 2017.
33. Bentaieb A, Hamarneh G. Adversarial stain transfer for histopathology image analysis. *IEEE Trans Med Imag.* 2018;37(3):792–802.
34. Shaban MT, Baur C, Navab N, Albarqouni S. Staingan: Stain style transfer for digital histological images. In: *2019 IEEE 16th International Symposium on Biomedical Imaging (ISBI 2019)*. IEEE; 2019:953-956.
35. Vasiljević J, Nisar Z, Feuerhake F, Wemmert C, Lampert T. CycleGAN for virtual stain transfer: is seeing really believing? *Artif Intell Med.* 2022;133:102420.
36. Fraggetta F, L'Imperio V, Ameisen D, et al. Best practice recommendations for the implementation of a digital pathology workflow in the anatomic pathology laboratory by the european society of digital and integrative pathology (ESDIP). *Diagnostics.* 2021;11(11):2167.
37. Kothari S, Phan JH, Wang MD. Eliminating tissue-fold artifacts in histopathological whole-slide images for improved image-based prediction of cancer grade. *J Pathol Inf.* 2013;4(1):22.
38. Avanaki ARN, Espig KS, Xthona A, Lanciault C, Kimpe TRL. Automatic image quality assessment for digital pathology. In: *Breast Imaging: 13th International Workshop, IWDM 2016, Malmö, Sweden, June 19-22, 2016, Proceedings 13*. Springer; 2016:431-438.
39. Hosseini MS, Zhang Y, Plataniotis KN. Encoding visual sensitivity by MaxPol convolution filters for image sharpness assessment. *IEEE Trans Image Process.* 2019;28(9):4510–4525.
40. Hosseini MS, Brawley-Hayes JAZ, Zhang Y, Chan L, Plataniotis KN, Damaskinos S. Focus quality assessment of high-throughput whole slide imaging in digital pathology. *IEEE Trans Med Imag.* 2020;39(1):62–74.
41. Gao D, Padfield D, Rittscher J, McKay R. Automated training data generation for microscopy focus classification. *International Conference on Medical Image Computing and Computer-Assisted Intervention*. Springer; 2010:446–453.
42. Palokangas S, Selinummi J, Yli-Harja O. Segmentation of folds in tissue section images. In: *2007 29th Annual International Conference of the IEEE Engineering in Medicine and Biology Society*. IEEE; 2007:5641-5644.
43. Kumar RR, Kumar VA, Kumar PNS, Sudhamony S, Ravindrakumar R. Detection and removal of artifacts in cervical cytology images using support vector machine. In: *2011 IEEE International Symposium on IT in Medicine and Education*. Vol 1. IEEE; 2011:717-721.
44. Shakhawat HM, Nakamura T, Kimura F, Yagi Y, Yamaguchi M. Automatic quality evaluation of whole slide images for the practical use of whole slide imaging scanner. *ITE Trans Media Technol Appl.* 2020;8(4):252–268.
45. Smit G, Ciompi F, Cigéhn M, Bodén A, Van Der Laak J, Mercan C. Quality control of whole-slide images through multi-class semantic segmentation of artifacts. In: *Medical Imaging with Deep Learning*. ; 2021.
46. Haghighat M, Browning L, Sirinukunwattana K, et al. Automated quality assessment of large digitised histology cohorts by artificial intelligence. *Sci Rep.* 2022;12(1):5002.
47. Janowczyk A, Zuo R, Gilmore H, Feldman M, Madabhushi A. HistoQC: an open-source quality control tool for digital pathology slides. *JCO Clin Cancer Inf.* 2019;3:1–7.
48. Weng Z, Seper A, Pryalukhin A, et al. GrandQC: a comprehensive solution to quality control problem in digital pathology. *Nat Commun.* 2024;15(1):10685.
49. Win KY, Choomchuay S. Automated segmentation of cell nuclei in cytology pleural fluid images using OTSU thresholding. *2017 International Conference on Digital Arts, Media and Technology (ICDAMT)*. IEEE; 2017:14–18.
50. Phoulady HA, Goldgof DB, Hall LO, Mouton PR. Nucleus segmentation in histology images with hierarchical multilevel thresholding. *Proc SPIE.* 2016;9791:979111.
51. Gao Y, Ratner V, Zhu L, et al. Hierarchical nucleus segmentation in digital pathology images. *Proc SPIE.* 2016;9791:304–309.
52. Xu H, Lu C, Berendt R, Jha N, Mandal M. Automatic nuclei detection based on generalized laplacian of Gaussian filters. *IEEE J Biomed Health Inf.* 2017;21(3):826–837.
53. Ghane N, Vard A, Talebi A, Nematollahy P. Segmentation of white blood cells from microscopic images using a novel combination of K-means clustering and modified watershed algorithm. *J Med Signals Sens.* 2017;7(2):92.
54. Zarei N, Bakhtiari A, Gallagher P, Keys M, MacAulay C. Automated prostate glandular and nuclei detection using hyperspectral imaging. In: *2017 IEEE 14th International Symposium on Biomedical Imaging (ISBI 2017)*. IEEE; 2017:1028-1031.
55. Lu C, Mahmood M, Jha N, Mandal M. A robust automatic nuclei segmentation technique for quantitative histopathological image analysis. *Anal Quant Cytol Histol.* 2012;34:296–308.
56. Veta M, Huisman A, Viergever MA, van Diest PJ, Pluim JPW. Marker-controlled watershed segmentation of nuclei in H&E stained breast cancer biopsy images. *2011 IEEE International Symposium on Biomedical Imaging: From Nano to Macro. IEEE*; 2011:618–621.
57. Koyuncu CF, Akhan E, Ersahin T, Cetin-Atalay R, Gunduz-Demir C. Iterative H-minima-based marker-controlled watershed for cell nucleus segmentation. *Cytom Part A.* 2016;89(4):338–349.
58. Rajyalakshmi U, Rao SK, Prasad KS. Supervised classification of breast cancer malignancy using integrated modified marker controlled watershed approach. In: *2017 IEEE 7th International Advance Computing Conference (IACC)*. IEEE; 2017:584-589.
59. Al-Kofahi Y, Lassoued W, Lee W, Roysam B. Improved automatic detection and segmentation of cell nuclei in histopathology images. *IEEE Trans Bio-Med Eng.* 2010;57(4):841–852.
60. Daněk O, Matula P, Ortiz-de-Solórzano C, Munoz-Barrutia A, Maška M, Kozubek M. Segmentation of touching cell nuclei using a two-stage graph cut model. *Scand Conf Image Anal.* 2009;5575:410–419.
61. Zhang L, Kong H, Chin CT, et al. Segmentation of cytoplasm and nuclei of abnormal cells in cervical cytology using global and local graph cuts. *Comput Med Imaging Graph.* 2014;38(5):369–380.
62. Wang C, Bu H, Bao J, Li C. A level set method for gland segmentation. In: *Proceedings of the IEEE Conference on Computer Vision and Pattern Recognition Workshops*. ; 2017:113-121.
63. Jia D, Zhang C, Wu N, Guo Z, Ge H. Multi-layer segmentation framework for cell nuclei using improved GVF snake model, watershed, and ellipse fitting. *Biomed Signal Process Control.* 2021;67:102516.
64. Graham S, Rajpoot NM. SAMS-NET: Stain-aware multi-scale network for instance-based nuclei segmentation in histology images. In: *2018 IEEE 15th International Symposium on Biomedical Imaging (ISBI 2018)*. IEEE; 2018:590-594.
65. Raza SEA, Cheung L, Shaban M, et al. Micro-Net: a unified model for segmentation of various objects in microscopy images. *Med Image Anal.* 2019;52:160–173.
66. Cui Y, Zhang G, Liu Z, Xiong Z, Hu J. A deep learning algorithm for one-step contour aware nuclei segmentation of histopathology images. *Med Biol Eng Comput.* 2019;57(9):2027–2043.
67. Zhou Y, Onder OF, Dou Q, Tsougenis E, Chen H, Heng PA. Cia-net: Robust nuclei instance segmentation with contour-aware information aggregation. In: *Information Processing in Medical Imaging: 26th International Conference*, IPMI 2019, Hong Kong, China, June 2–7, 2019, Proceedings 26. Springer; 2019:682-693.
68. Zhang D, Song Y, Liu S, Feng D, Wang Y, Cai W. Nuclei instance segmentation with dual contour-enhanced adversarial network. In: *2018 IEEE 15th International Symposium on Biomedical Imaging (ISBI 2018)*. IEEE; 2018:409-412.
69. Schmidt U, Weigert M, Broaddus C, Myers G. Cell detection with star-convex polygons. In: *Medical Image Computing and Computer Assisted Intervention–MICCAI 2018: 21st International Conference, Granada, Spain, September 16-20, 2018, Proceedings, Part II 11*. Springer; 2018:265-273.
70. Graham S, Vu QD, Raza SEA, et al. Hover-Net: simultaneous segmentation and classification of nuclei in multi-tissue histology images. *Med Image Anal.* 2019;58:101563.
71. Naylor P, Laé M, Reyal F, Walter T. Segmentation of nuclei in histopathology images by deep regression of the distance map. *IEEE Trans Med Imag.* 2019;38(2):448–459.
72. Chen S, Ding C, Liu M, Cheng J, Tao D. CPP-Net: context-aware polygon proposal network for nucleus segmentation. *IEEE Trans Image Process.* 2023;32:980–994.
73. Stringer C, Wang T, Michaelos M, Pachitariu M. Cellpose: a generalist algorithm for cellular segmentation. *Nat Methods.* 2021;18(1):100–106.

74. Jiang H, Zhang R, Zhou Y, Wang Y, Chen H. Donet: Deep de-overlapping network for cytology instance segmentation. In: *Proceedings of the IEEE/CVF Conference on Computer Vision and Pattern Recognition*. ; 2023:15641-15650.
75. Liu X, Wang S, Lin JCW, Liu S. An algorithm for overlapping chromosome segmentation based on region selection. *Neural Comput Appl.* 2024;36(1):133–142.
76. Song Y, Tan EL, Jiang X, et al. Accurate cervical cell segmentation from overlapping clumps in pap smear images. *IEEE Trans Med Imag.* 2017;36(1):288–300.
77. Tareef A, Song Y, Huang H, et al. Optimizing the cervix cytological examination based on deep learning and dynamic shape modeling. *Neurocomputing.* 2017;248:28–40.
78. Fan X, Liu H, Zheng H, Zhai J, Zhang L. DaCSeg: divide and conquer for accurate overlapping chromosome instance segmentation in metaphase cell images. *Biomed Signal Process Control.* 2024;89:105880.
79. Bertram CA, Aubreville M, Marzahl C, Maier A, Klopfleisch R. A large-scale dataset for mitotic figure assessment on whole slide images of canine cutaneous mast cell tumor. *Sci Data.* 2019;6(1):274.
80. Ma J, Xie R, Ayyadhury S, et al. The multimodality cell segmentation challenge: toward universal solutions. *Nat Methods.* 2024;21(6):1103–1113.
81. Cireşan DC, Giusti A, Gambardella LM, Schmidhuber J. Mitosis detection in breast cancer histology images with deep neural networks. *International Conference on Medical Image Computing and Computer-Assisted Intervention*. Springer Berlin Heidelberg; 2013:411–418.
82. Chen H, Wang X, Heng PA. Automated mitosis detection with deep regression networks. In: *2016 IEEE 13th International Symposium on Biomedical Imaging (ISBI)*. IEEE; 2016:1204-1207.
83. Albayrak A, Bilgin G. Mitosis detection using convolutional neural network based features. In: *2016 IEEE 17th International Symposium on Computational Intelligence and Informatics (CINTI)*. IEEE; 2016:335-340.
84. Rao S. Mitos-rcnn: A novel approach to mitotic figure detection in breast cancer histopathology images using region based convolutional neural networks. *arXiv preprint arXiv:180701788*. Published online 2018.
85. Li C, Wang X, Liu W, Latecki LJ. DeepMitosis: mitosis detection via deep detection, verification and segmentation networks. *Med Image Anal.* 2018;45:121–133.
86. Mahmood T, Arsalan M, Owais M, Lee MB, Park KR. Artificial intelligence-based mitosis detection in breast cancer histopathology images using faster R-CNN and deep CNNs. *J Clin Med.* 2020;9(3):749.
87. Yoo I, Yoo D, Paeng K. Pseudoedgenet: Nuclei segmentation only with point annotations. In: *Medical Image Computing and Computer Assisted Intervention–MICCAI 2019: 22nd International Conference, Shenzhen, China, October 13–17, 2019, Proceedings, Part I 22*. Springer; 2019:731-739.
88. Qu H, Wu P, Huang Q, et al. Weakly supervised deep nuclei segmentation using partial points annotation in histopathology images. *IEEE Trans Med Imag.* 2020;39(11):3655–3666.
89. Qu H, Yi J, Huang Q, Wu P, Metaxas D. Nuclei segmentation using mixed points and masks selected from uncertainty. In: *2020 IEEE 17th International Symposium on Biomedical Imaging (ISBI)*. IEEE; 2020:973-976.
90. Tian K, Zhang J, Shen H, et al. Weakly-supervised nucleus segmentation based on point annotations: A coarse-to-fine self-stimulated learning strategy. In: *Medical Image Computing and Computer Assisted Intervention–MICCAI 2020: 23rd International Conference, Lima, Peru, October 4–8, 2020, Proceedings, Part V 23*. Springer; 2020:299-308.
91. Lou W, Li H, Li G, Han X, Wan X. Which pixel to annotate: a label-efficient nuclei segmentation framework. *IEEE Trans Med Imag.* 2023;42(4):947–958.
92. Zheng X, Wang Y, Wang G, Liu J. Fast and robust segmentation of white blood cell images by self-supervised learning. *Micron.* 2018;107:55–71.
93. Sahasrabudhe M, Christodoulidis S, Salgado R, et al. Self-supervised nuclei segmentation in histopathological images using attention. In: *Medical Image Computing and Computer Assisted Intervention–MICCAI 2020: 23rd International Conference, Lima, Peru, October 4–8, 2020, Proceedings, Part V 23*. Springer; 2020:393-402.
94. Hsu J, Chiu W, Yeung S. DARCNN: Domain Adaptive Region-based Convolutional Neural Network for Unsupervised Instance Segmentation in Biomedical Images. *2021 IEEE/CVF Conference on Computer Vision and Pattern Recognition (CVPR)*. 2021; 2021:1003–1012.
95. Ali H, Elattar M, Selim S. A multi-scale self-supervision method for improving cell nuclei segmentation in pathological tissues. *Med Image Underst Anal.* 2022;13413:751–763.
96. Punn NS, Agarwal S. BT-Unet: a self-supervised learning framework for biomedical image segmentation using Barlow twins with U-net models. *Mach Learn.* 2022;111(12):4585–4600.
97. Liu D, Zhang D, Song Y, et al. Unsupervised instance segmentation in microscopy images via panoptic domain adaptation and task re-weighting. In: *Proceedings of the IEEE/CVF Conference on Computer Vision and Pattern Recognition*. ; 2020:4243-4252.
98. Xie X, Chen J, Li Y, Shen L, Ma K, Zheng Y. Instance-aware self-supervised learning for nuclei segmentation. In: *Medical Image Computing and Computer Assisted Intervention–MICCAI 2020: 23rd International Conference, Lima, Peru, October 4–8, 2020, Proceedings, Part V 23*. Springer; 2020:341-350.
99. Graham S, Epstein D, Rajpoot N. Dense steerable filter CNNs for exploiting rotational symmetry in histology images. *IEEE Trans Med Imag.* 2020;39(12):4124–4136.
100. Upschulte E, Harmeling S, Amunts K, Dickscheid T. Uncertainty-aware contour proposal networks for cell segmentation in multi-modality high-resolution microscopy images. In: *Competitions in Neural Information Processing Systems*. PMLR. 2023:1–12.
101. Cutler KJ, Stringer C, Lo TW, et al. Omnipose: a high-precision morphology-independent solution for bacterial cell segmentation. *Nat Methods.* 2022;19(11):1438–1448.
102. Qaiser T, Tsang YW, Taniyama D, et al. Fast and accurate tumor segmentation of histology images using persistent homology and deep convolutional features. *Med Image Anal.* 2019;55:1–14.
103. Zeng L, Tang H, Wang W, et al. MAMC-Net: an effective deep learning framework for whole-slide image tumor segmentation. *Multimed Tools Appl.* 2023;82(25):39349–39369.
104. Wang H, Xian M, Vakanski A. Ta-net: Topology-aware network for gland segmentation. In: *Proceedings of the IEEE/CVF Winter Conference on Applications of Computer Vision*. ; 2022:1556-1564.
105. Chen H, Qi X, Yu L, Heng PA. DCAN: deep contour-aware networks for accurate gland segmentation. In: *Proceedings of the IEEE Conference on Computer Vision and Pattern Recognition*. ; 2016:2487-2496.
106. Mei L, Guo X, Huang X, Weng Y, Liu S, Lei C. Dense contour-imbalance aware framework for colon gland instance segmentation. *Biomed Signal Process Control.* 2020;60:101988.
107. Yi F, Yang L, Wang S, et al. Microvessel prediction in H&E stained pathology images using fully convolutional. *Neural Netw BMC Bioinf.* 2018;19(1):64.
108. Li X, Tang Q, Yu J, Wang Y, Shi Z. Microvascularity detection and quantification in glioma: a novel deep-learning-based framework. *Lab Invest.* 2019;99(10):1515–1526.
109. Xu J, Cai C, Zhou Y, et al. Multi-tissue partitioning for whole slide images of colorectal cancer histopathology images with deeptissue net. In: *Digital Pathology: 15th European Congress, ECDP 2019, Warwick, UK, April 10–13, 2019, Proceedings 15*. Springer; 2019:100-108.
110. Wetteland R, Engan K, Eftestøl T, Kvikstad V, Janssen EAM. A multiscale approach for whole-slide image segmentation of five tissue classes in urothelial carcinoma slides. *Technol Cancer Res Treat.* 2020:19.
111. Van Rijthoven M, Balkenhol M, Siliņa K, Van Der Laak J, Ciompi F. HookNet: multi-resolution convolutional neural networks for semantic segmentation in histopathology whole-slide images. *Med Image Anal.* 2021;68:101890.
112. Xu G, Song Z, Sun Z, et al. Camel: A weakly supervised learning framework for histopathology image segmentation. In: *Proceedings of the IEEE/CVF International Conference on Computer Vision*. ; 2019:10682-10691.
113. Chan L, Hosseini MS, Rowsell C, Plataniotis KN, Damaskinos S. Histosegnet: Semantic segmentation of histological tissue type in whole slide images. In: *Proceedings of the IEEE/CVF International Conference on Computer Vision*. ; 2019:10662-10671.
114. Zhong L, Wang G, Liao X, Zhang S. HAMIL: high-resolution activation maps and interleaved learning for weakly supervised segmentation of histopathological images. *IEEE Trans Med Imag.* 2023;42(10):2912–2923.
115. Xu H, Lu C, Berendt R, Jha N, Mandal M. Automated analysis and classification of melanocytic tumor on skin whole slide images. *Comput Med Imaging Graph.* 2018;66:124–134.
116. Lu C, Mandal M. Automated analysis and diagnosis of skin melanoma on whole slide histopathological images. *Pattern Recognit.* 2015;48(8):2738–2750.

117. Jiao L, Chen Q, Li S, Xu Y. Colon cancer detection using whole slide histopathological images. *World Congr Med Phys Biomed Eng.* 2013;39:1283–1286.
118. Nguyen K, Jain AK, Sabata B. Prostate cancer detection: fusion of cytological and textural features. *J Pathol Inf.* 2012;2(2):3.
119. Basavanhally A, Ganesan S, Agner S, et al. Computerized image-based detection and grading of lymphocytic infiltration in HER2. Breast cancer histopathology. *IEEE Trans Bio-Med Eng.* 2010;57(3):642–653.
120. Huang PW, Lai YH. Effective segmentation and classification for HCC biopsy images. *Pattern Recognit.* 2010;43(4):1550–1563.
121. Krizhevsky A, Sutskever I, Hinton GE. ImageNet classification with deep convolutional. *Neural Netw Commun Acm.* 2017;60(6):84–90.
122. He K, Zhang X, Ren S, Sun J. Deep residual learning for image recognition. In: *Proceedings of the IEEE Conference on Computer Vision and Pattern Recognition.* ; 2016:770-778.
123. Hou L, Samaras D, Kurc TM, Gao Y, Davis JE, Saltz JH. Patch-based convolutional neural network for whole slide tissue image classification. In: *Proceedings of the IEEE Conference on Computer Vision and Pattern Recognition.* ; 2016:2424-2433.
124. Sharma H, Zerbe N, Klempert I, Hellwich O, Hufnagl P. Deep convolutional neural networks for histological image analysis in gastric carcinoma whole slide images. *Diagn Pathol.* 2016;1(8):13.
125. Wang D, Khosla A, Gargeya R, Irshad H, Beck AH. Deep learning for identifying metastatic breast cancer. *arXiv preprint arXiv:160605718*. Published online 2016.
126. Lin H, Chen H, Dou Q, Wang L, Qin J, Heng PA. Scannet: A fast and dense scanning framework for metastastic breast cancer detection from whole-slide image. In: *2018 IEEE Winter Conference on Applications of Computer Vision (WACV)*. IEEE; 2018:539-546.
127. Naik N, Madani A, Esteva A, et al. Deep learning-enabled breast cancer hormonal receptor status determination from base-level H&E stains. *Nat Commun.* 2020;11(1):5727.
128. Li B, Li Y, Eliceiri KW. Dual-stream multiple instance learning network for whole slide image classification with self-supervised contrastive learning. In: *Proceedings of the IEEE/CVF Conference on Computer Vision and Pattern Recognition.* ; 2021:14318-14328.
129. Lu MY, Chen RJ, Wang J, Dillon D, Mahmood F. Semi-supervised histology classification using deep multiple instance learning and contrastive predictive coding. *arXiv preprint arXiv:191010825*. Published online 2019.
130. Huang SJ, Gao W, Zhou ZH. Fast multi-instance multi-label learning. *IEEE Trans Pattern Anal Mach Intell.* 2019;41(11):2614–2627.
131. Pinheiro PO, Collobert R. From image-level to pixel-level labeling with convolutional networks. In: *Proceedings of the IEEE Conference on Computer Vision and Pattern Recognition.* ; 2015:1713-1721.
132. Ilse M, Tomczak J, Welling M. Attention-based deep multiple instance learning. In: *International Conference on Machine Learning. PMLR.* 2018:2127–2136.
133. Lu MY, Williamson DFK, Chen TY, Chen RJ, Barbieri M, Mahmood F. Data-efficient and weakly supervised computational pathology on whole-slide images. *Nat Biomed Eng.* 2021;5(6):555–570.
134. Shao Z, Bian H, Chen Y, et al. TransMIL: transformer based correlated multiple instance learning for whole slide image classification. *Adv Neural Inf Process Syst.* 2021;34:2136–2147.
135. Kipf TN, Welling M. Semi-supervised classification with graph convolutional networks. *arXiv preprint arXiv:160902907*. Published online 2016.
136. Chen RJ, Lu MY, Shaban M, et al. Whole slide images are 2d point clouds: Context-aware survival prediction using patch-based graph convolutional networks. In: *Medical Image Computing and Computer Assisted Intervention–MICCAI 2021: 24th International Conference, Strasbourg, France, September 27–October 1, 2021, Proceedings, Part VIII 24*. Springer; 2021:339-349.
137. Pati P, Jaume G, Foncubierta-Rodríguez A, et al. Hierarchical graph representations in digital pathology. *Med Image Anal.* 2022;75:102264.
138. Lu W, Toss M, Dawood M, Rakha E, Rajpoot N, Minhas F. SlideGraph +: whole slide image level graphs to predict HER2 status in breast cancer. *Med Image Anal.* 2022;80:102486.
139. Chen Z, Zhang J, Che S, Huang J, Han X, Yuan Y. Diagnose like a pathologist: weakly-supervised pathologist-tree network for slide-level immunohistochemical scoring. *Proc AAAI Conf Artif Intell.* 2021;35:47–54.
140. Hou W, Huang H, Peng Q, Yu R, Yu L, Wang L. Spatial-hierarchical graph neural network with dynamic structure learning for histological image classification. *International Conference on Medical Image Computing and Computer-Assisted Intervention*. Springer; 2022:181–191.
141. Hou W, Yu L, Lin C, et al. H^2-MIL: exploring hierarchical representation with heterogeneous multiple instance learning for whole slide image analysis. *Proc AAAI Conf Artif Intell.* 2022;36:933–941.
142. Bontempo G, Porrello A, Bolelli F, Calderara S, Ficarra E. DAS-MIL: distilling across scales for MIL classification of histological WSIs. In: *International Conference on Medical Image Computing and Computer-Assisted Intervention*. Springer; 2023:248-258.
143. Klimov S, Miligy IM, Gertych A, et al. A whole slide image-based machine learning approach to predict ductal carcinoma in situ (DCIS) recurrence risk. *Breast Cancer Res.* 2019;21(1):83.
144. Zheng Q, Jiang Z, Ni X, et al. Machine learning quantified tumor-stroma ratio is an independent prognosticator in muscle-invasive bladder cancer. *Int J Mol Sci.* 2023;24(3):2746.
145. Li H, Wang J, Li Z, et al. Deep learning-based pathology image analysis enhances magee feature correlation with oncotype DX breast recurrence score. *Front Med.* 2022;9:886763.
146. Bhargava HK, Leo P, Elliott R, et al. Computationally derived image signature of stromal morphology is prognostic of prostate cancer recurrence following prostatectomy in African American patients. *Clin Cancer Res.* 2020;26(8):1915–1923.
147. Wang X, Chen Y, Gao Y, et al. Predicting gastric cancer outcome from resected lymph node histopathology images using deep learning. *Nat Commun.* 2021;12(1):1637.
148. Murchan P, Ó'Brien C, O'Connell S, et al. Deep learning of histopathological features for the prediction of tumour molecular genetics. *Diagnostics.* 2021;11(8):1406.
149. Mou T, Liang J, Vu TN, Tian M, Gao Y. A comprehensive landscape of imaging feature-associated RNA expression profiles in human breast tissue. *Sensors.* 2023;23(3):1432.
150. Loeffler CML, OrtizBruechle N, Jung M, et al. Artificial intelligence-based detection of FGFR3 mutational status directly from routine histology in bladder cancer: a possible preselection for molecular testing? *Eur Urol Focus.* 2022;8(2):472–479.
151. Guitton T, Allaume P, Rabilloud N, et al. Artificial intelligence in predicting microsatellite instability and KRAS, BRAF mutations from whole-slide images in colorectal cancer: a systematic review. *Diagnostics.* 2023;14(1):99.
152. Wang X, Zou C, Zhang Y, et al. Prediction of BRCA gene mutation in breast cancer based on deep learning and histopathology images. *Front Genet.* 2021;12:661109.
153. Anand D, Kurian NC, Dhage S, et al. Deep learning to estimate human epidermal growth factor receptor 2 status from hematoxylin and eosin-stained breast tissue images. *J Pathol Inf.* 2020;11(1):19.
154. Zhang H, Kalirai H, Acha-Sagredo A, Yang X, Zheng Y, Coupland SE. Piloting a deep learning model for predicting nuclear BAP1 immunohistochemical expression of uveal melanoma from hematoxylin-and-eosin sections. *Transl Vis Sci Technol.* 2020;9(2):50.
155. Bourgade R, Rabilloud N, Perennec T, et al. Deep learning for detecting BRCA mutations in high-grade ovarian cancer based on an innovative tumor segmentation method from whole slide images. *Mod Pathol.* 2023;36(11):100304.
156. Kather JN, Pearson AT, Halama N, et al. Deep learning can predict microsatellite instability directly from histology in gastrointestinal cancer. *Nat Med.* 2019;25(7):1054–1056.
157. Echle A, Grabsch HI, Quirke P, et al. Clinical-grade detection of microsatellite instability in colorectal tumors by deep learning. *Gastroenterology.* 2020;159(4):1406–1416.e11.
158. Zhu X, Yao J, Zhu F, Huang J. Wsisa: Making survival prediction from whole slide histopathological images. In: *Proceedings of the IEEE Conference on Computer Vision and Pattern Recognition.* ; 2017:7234-7242.
159. Fan L, Sowmya A, Meijering E, Song Y. Learning visual features by colorization for slide-consistent survival prediction from whole slide images. In: *Medical Image Computing and Computer Assisted Intervention–MICCAI 2021: 24th International Conference, Strasbourg, France, September 27–October 1, 2021, Proceedings, Part VIII 24*. Springer; 2021:592-601.

160. Fan L, Sowmya A, Meijering E, Song Y. Cancer survival prediction from whole slide images with self-supervised learning and slide consistency. *IEEE Trans Med Imag.* 2023;42(5):1401–1412.
161. Chen C, Cao Y, Li W, et al. The pathological risk score: a new deep learning-based signature for predicting survival in cervical cancer. *Cancer Med.* 2023;12(2):1051–1063.
162. Murchan P, Baird AM, ÓBroin P, Sheils O, Finn SP. Surrogate biomarker prediction from whole-slide images for evaluating overall survival in lung adenocarcinoma. *Diagnostics.* 2024;14(5):462.
163. Liu P, Ji L, Ye F, Fu B. AdvMIL: adversarial multiple instance learning for the survival analysis on whole-slide images. *Med Image Anal.* 2024;91:103020.
164. Di D, Li S, Zhang J, Gao Y. Ranking-based survival prediction on histopathological whole-slide images. I*nternational Conference on Medical Image Computing and Computer-Assisted Intervention*. Springer; 2020:428–438.
165. Jiang S, Suriawinata AA, Hassanpour S. MHAttnSurv: multi-head attention for survival prediction using whole-slide pathology images. *Comput Biol Med.* 2023;158:106883.
166. Liu P, Fu B, Ye F, Yang R, Ji L. DSCA: a dual-stream network with cross-attention on whole-slide image pyramids for cancer prognosis. *Expert Syst Appl.* 2023;227:120280.
167. Shen Y, Liu L, Tang Z, et al. Explainable survival analysis with convolution-involved vision transformer. *Proc AAAI Conf Artif Intell.* 2022;36:2207–2215.
168. Liang J, Zhang W, Yang J, et al. Deep learning supported discovery of biomarkers for clinical prognosis of liver cancer. *Nat Mach Intell.* 2023;5(4):408–420.
169. Mobadersany P, Yousefi S, Amgad M, et al. Predicting cancer outcomes from histology and genomics using convolutional networks. *Proc Natl Acad Sci.* 2018;115(13):E2970–E2979.
170. Peng Y, Chu Y, Chen Z, et al. Combining texture features of whole slide images improves prognostic prediction of recurrence-free survival for cutaneous melanoma patients. *World J Surg Oncol.* 2020;18(1):130.
171. Rathore FA, Khan HS, Ali HM, et al. Survival prediction of glioma patients from integrated radiology and pathology images using machine learning ensemble regression methods. *Appl Sci.* 2022;12(20):10357.
172. Yu YC, Shi TM, Gu SL, et al. A novel cervix carcinoma biomarker: pathological-epigenomics, integrated analysis of MethylMix algorithm and pathology for predicting response to cancer immunotherapy. *Front Oncol.* 2022;12:1053800.
173. Chen RJ, Lu MY, Wang J, et al. Pathomic fusion: an integrated framework for fusing histopathology and genomic features for cancer diagnosis and prognosis. *IEEE Trans Med Imag.* 2022;41(4):757–770.
174. Braman N, Gordon JWH, Goossens ET, Willis C, Stumpe MC, Venkataraman J. Deep orthogonal fusion: multimodal prognostic biomarker discovery integrating radiology, pathology, genomic, and clinical data. In: *Medical Image Computing and Computer Assisted Intervention–MICCAI 2021: 24th International Conference, Strasbourg, France, September 27–October 1, 2021, Proceedings, Part V 24*. Springer; 2021:667-677.
175. Wu X, Shi Y, Wang M, Li A. CAMR: cross-aligned multimodal representation learning for cancer survival prediction. *Bioinformatics.* 2023;39(1) btad025.
176. Wang Z, Li R, Wang M, Li A. GPDBN: deep bilinear network integrating both genomic data and pathological images for breast cancer prognosis prediction. *Bioinformatics.* 2021;37(18):2963–2970.
177. Li R, Wu X, Li A, Wang M. HFBSurv: hierarchical multimodal fusion with factorized bilinear models for cancer survival prediction. *Bioinformatics.* 2022;38(9):2587–2594.
178. Wang Y, Luo Y, Li B, Shen X. Multi-modality fusion based lung cancer survival analysis with self-supervised whole slide image representation learning. *Pattern Recognit Comput Vis.* 2024;14437:333–345.
179. Li C, Zhu X, Yao J, Huang J. Hierarchical transformer for survival prediction using multimodality whole slide images and genomics. In: *2022 26th International Conference on Pattern Recognition (ICPR)*. IEEE; 2022:4256-4262.
180. Chen RJ, Lu MY, Weng WH, et al. Multimodal co-attention transformer for survival prediction in gigapixel whole slide images. In: *Proceedings of the IEEE/CVF International Conference on Computer Vision.* ; 2021:4015-4025.
181. Li Z, Jiang Y, Lu M, Li R, Xia Y. Survival prediction via hierarchical multimodal co-attention transformer: a computational histology-radiology solution. *IEEE Trans Med Imag.* 2023;42(9):2678–2689.
182. Jaume G, Vaidya A, Chen RJ, Williamson DFK, Liang PP, Mahmood F. Modeling dense multimodal interactions between biological pathways and histology for survival prediction. In: *Proceedings of the IEEE/CVF Conference on Computer Vision and Pattern Recognition*. ; 2024:11579-11590.
183. Liu H, Shi Y, Li A, Wang M. Multi-modal fusion network with intra- and inter-modality attention for prognosis prediction in breast cancer. *Comput Biol Med.* 2024;168:107796.
184. Kirillov A, Mintun E, Ravi N, et al. Segment anything. In: *Proceedings of the IEEE/CVF International Conference on Computer Vision*. ; 2023:4015-4026.
185. Radford A, Kim JW, Hallacy C, et al. Learning transferable visual models from natural language supervision. In: *International Conference on Machine Learning*. PmLR. 2021:8748–8763.
186. Radford A, Narasimhan K, Salimans T, Sutskever I. Improving Language Understanding by Generative Pre-Training.
187. Brown T, Mann B, Ryder N, et al. Language models are few-shot learners. *Adv Neural Inf Process Syst.* 2020;33:1877–1901.
188. Vorontsov E, Bozkurt A, Casson A, et al. A foundation model for clinical-grade computational pathology and rare cancers detection. *Nat Med.* 2024;30(10):2924–2935.
189. Campanella G, Kwan R, Fluder E, et al. Computational Pathology at Health System Scale–Self-Supervised Foundation Models from Three Billion Images. *arXiv preprint arXiv:231007033*. Published online 2023.
190. Chen RJ, Ding T, Lu MY, et al. Towards a general-purpose foundation model for computational pathology. *Nat Med.* 2024;30(3):850–862.
191. Dippel J, Feulner B, Winterhoff T, et al. RudolfV: a foundation model by pathologists for pathologists. *arXiv preprint arXiv:240104079*. Published online 2024.
192. Xu H, Usuyama N, Bagga J, et al. A whole-slide foundation model for digital pathology from real-world data. *Nature.* 2024;630(8015):181–188.
193. Ciga O, Xu T, Martel AL. Self supervised contrastive learning for digital histopathology. *Mach Learn Appl.* 2022;7:100198.
194. Huang Z, Bianchi F, Yuksekgonul M, Montine TJ, Zou J. A visual-language foundation model for pathology image analysis using medical twitter. *Nat Med.* 2023;29(9):2307–2316.
195. Oluchi Ikezogwo W, Saygin Seyfioglu M, Ghezloo F, et al. Quilt-1M: One Million Image-Text Pairs for Histopathology. *arXiv e-prints*. Published online 2023:arXiv-2306.
196. Lu MY, Chen B, Williamson DFK, et al. A visual-language foundation model for computational pathology. *Nat Med.* 2024;30(3):863–874.
197. Dosovitskiy A, Beyer L, Kolesnikov A, et al. An Image is Worth 16x16 Words: Transformers for Image Recognition at Scale. *International Conference on Learning Representations*. 2020.
198. Filiot A, Ghermi R, Olivier A, et al. Scaling self-supervised learning for histopathology with masked image modeling. *medRxiv.* 2023;2023 07.21,23292757.
199. He K, Fan H, Wu Y, Xie S, Girshick R. Momentum contrast for unsupervised visual representation learning. In: *Proceedings of the IEEE/CVF Conference on Computer Vision and Pattern Recognition*. ; 2020:9729-9738.
200. Chen T, Kornblith S, Norouzi M, Hinton G. A simple framework for contrastive learning of visual representations. In: *International Conference on Machine Learning*. PmLR. 2020:1597–1607.
201. Oquab M, Darcet T, Moutakanni T, et al. DINOv2: learning robust visual features without supervision. *Trans Mach Learn Res.* 2024.
202. Xun D, Wang R, Zhang X, Wang Y. Microsnoop: a generalist tool for microscopy image representation. *Innovation.* 2024;5(1):100541.
203. Wang X, Du Y, Yang S, et al. RetCCL: clustering-guided contrastive learning for whole-slide image retrieval. *Med Image Anal.* 2023;83:102645.
204. Wang X, Yang S, Zhang J, et al. Transformer-based unsupervised contrastive learning for histopathological image classification. *Med Image Anal.* 2022;81:102559.
205. Wang X, Zhao J, Marostica E, et al. A pathology foundation model for cancer diagnosis and prognosis prediction. *Nature.* 2024;634(8035):970–978.
206. Kang M, Song H, Park S, Yoo D, Pereira S. Benchmarking self-supervised learning on diverse pathology datasets. In: *Proceedings of the IEEE/CVF Conference on Computer Vision and Pattern Recognition*. ; 2023:3344-3354.
207. Sun Y, Zhu C, Zheng S, et al. PathAsst: a generative foundation ai assistant towards artificial general intelligence of pathology. *Proc AAAI Conf Artif Intell.* 2024;38:5034–5042.

208. Sun Y, Si Y, Zhu C, et al. CPath-Omni: A Unified Multimodal Foundation Model for Patch and Whole Slide Image Analysis in Computational Pathology. *arXiv preprint arXiv:241212077*. Published online 2024.
209. Devlin J, Chang MW, Lee K, Toutanova K. Bert: Pre-training of deep bidirectional transformers for language understanding. In: *Proceedings of the 2019 Conference of the North American Chapter of the Association for Computational Linguistics: Human Language Technologies, Volume 1 (Long and Short Papers)*. ; 2019:4171-4186.
210. Luo R, Sun L, Xia Y, et al. BioGPT: generative pre-trained transformer for biomedical text generation and mining. *Brief Bioinf.* 2022;23(6) bbac409.
211. He K, Chen X, Xie S, Li Y, Dollár P, Girshick R. Masked autoencoders are scalable vision learners. In: *Proceedings of the IEEE/CVF Conference on Computer Vision and Pattern Recognition*. ; 2022:16000-16009.
212. Zhou J, Wei C, Wang H, et al. Image BERT Pre-Training with Online Tokenizer. In: Proceedings of the International Conference on Learning Representations; 2022.
213. Yu J, Wang Z, Vasudevan V, Yeung L, Seyedhosseini M, Wu Y. CoCa: contrastive captioners are image-text foundation models. *Trans Mach Learn Res.* 2022.
214. Lu MY, Chen B, Williamson DFK, et al. A multimodal generative AI copilot for human pathology. *Nature.* 2024;634(8033):466–473.
215. Shaikovski G, Casson A, Severson K, et al. Prism: A multi-modal generative foundation model for slide-levelhistopathology. *arXiv preprint arXiv:240510254*. Published online 2024.
216. Ding T, Wagner SJ, Song AH, et al. Multimodal whole slide foundation model for pathology. *arXiv preprint arXiv:241119666*. Published online 2024.
217. Salimans T, Goodfellow I, Zaremba W, Cheung V, Radford A, Chen X. Improved techniques for training GANs. In: *Proceedings of the 30th International Conference on Neural Information Processing Systems*. ; 2016:2234-2242.
218. Heusel M, Ramsauer H, Unterthiner T, Nessler B, Hochreiter S. GANs trained by a two time-scale update rule converge to a local nash equilibrium. In: *Proceedings of the 31st International Conference on Neural Information Processing Systems*. ; 2017:6629-6640.
219. Papineni K, Roukos S, Ward T, Zhu WJ. Bleu: a method for automatic evaluation of machine translation. In: *Proceedings of the 40th Annual Meeting of the Association for Computational Linguistics*. ; 2002:311-318.
220. Lin CY. Rouge: A package for automatic evaluation of summaries. In: *Text Summarization Branches Out*. ; 2004:74-81.
221. Hore A, Ziou D. Image quality metrics: PSNR vs. SSIM. In: *2010 20th International Conference on Pattern Recognition*. IEEE; 2010:2366-2369.
222. Xu Z, Huang X, Moro CF, Bozóky B, Zhang Q. GAN-based virtual re-staining: a promising solution for whole slide image analysis. *arXiv preprint arXiv:190104059*. Published online 2019.
223. He Y, Liu Z, Qi M, et al. PST-diff: achieving high-consistency stain transfer by diffusion models with pathological and structural constraints. *IEEE Trans Med Imag.* 2024;43(10):3634–3647.
224. Lin Y, Zeng B, Wang Y, et al. Unpaired multi-domain stain transfer for kidney histopathological images. *Proc AAAI Conf Artif Intell.* 2022;36:1630–1637.
225. Liu S, Zhang B, Liu Y, et al. Unpaired stain transfer using pathology-consistent constrained generative adversarial networks. *IEEE Trans Med Imag.* 2021;40(8):1977–1989.
226. Kataria T, Knudsen B, Elhabian SY. StainDiffuser: multitask dual diffusion model for virtual staining. *arXiv preprint arXiv:240311340*. Published online 2024.
227. Dubey S, Chong Y, Knudsen B, Elhabian SY. VIMs: virtual immunohistochemistry multiplex staining via text-to-stain diffusion trained on uniplex stains. *Mach Learn Med Imaging.* 2025:143–155.
228. Pati P, Karkampouna S, Bonollo F, et al. Accelerating histopathology workflows with generative AI-based virtually multiplexed tumour profiling. *Nat Mach Intell.* 2024;6(9):1077–1093.
229. Croce AC, Bottiroli G. Autofluorescence spectroscopy and imaging: a tool for biomedical research and diagnosis. *Eur J Histochem: EJH.* 2014;58(4):2461.
230. Rivenson Y, De Haan K, Wallace WD, Ozcan A. Emerging advances to transform histopathology using virtual staining. *BME Front.* 2020;2020:9647163.
231. Zhang Y, de Haan K, Rivenson Y, Li J, Delis A, Ozcan A. Digital synthesis of histological stains using micro-structured and multiplexed virtual staining of label-free tissue. *Light: Sci Appl.* 2020;9(1):78.
232. Pillar N, Ozcan A. Virtual tissue staining in pathology using machine learning. *Expert Rev Mol Diagn.* 2022;22(11):987–989.
233. Chen Z, Guo X, Yang C, Ibragimov B, Yuan Y. Joint spatial-wavelet dual-stream network for super-resolution. In: *Medical Image Computing and Computer Assisted Intervention–MICCAI 2020: 23rd International Conference, Lima, Peru, October 4–8, 2020, Proceedings, Part V 23*. Springer; 2020:184-193.
234. Li B, Keikhosravi A, Loeffler AG, Eliceiri KW. Single image super-resolution for whole slide image using convolutional neural networks and self-supervised color normalization. *Med Image Anal.* 2021;68:101938.
235. Wu X, Chen Z, Peng C, Ye X. MMSRNet: pathological image super-resolution by multi-task and multi-scale learning. *Biomed Signal Process Control.* 2023;81:104428.
236. Ma J, Yu J, Liu S, et al. PathSRGAN: multi-supervised super-resolution for cytopathological images using generative adversarial network. *IEEE Trans Med Imag.* 2020;39(9):2920–2930.
237. Chen Z, Wang J, Jia C, Ye X. Pathological image super-resolution using mix-attention generative adversarial network. *Int J Mach Learn Cybern.* 2024;15(1):149–159.
238. Xu X, Kapse S, Prasanna P. Histo-Diffusion: A Diffusion Super-Resolution Method for Digital Pathology with Comprehensive Quality Assessment. *arXiv preprint arXiv:240815218*. Published online 2024.
239. Yang Z, Chen H, Qian Z, et al. Region attention transformer for medical image restoration. *International Conference on Medical Image Computing and Computer-Assisted Intervention*. Springer; 2024:603–613.
240. Chen W, Liu J, Chow TWS, Yuan Y. STAR-RL: spatial-temporal hierarchical reinforcement learning for interpretable pathology image super-resolution. *IEEE Trans Med Imag.* 2024;43(12):4368–4379.
241. Benito-Del-Valle L, Alvarez-Gila A, Eguskiza I, Saratxaga CL. Unleashing the Potential of Synthetic Images: A Study on Histopathology Image Classification. *arXiv preprint arXiv:240916002*. Published online 2024.
242. Levine AB, Peng J, Farnell D, et al. Synthesis of diagnostic quality cancer pathology images by generative adversarial networks. *J Pathol.* 2020;252(2):178–188.
243. Gullapally SC, Zhang Y, Mittal NK, et al. Synthetic DOmain-Targeted Augmentation (S-DOTA) improves model generalization in digital pathology. *arXiv preprint arXiv:230502401*. Published online 2023.
244. Liu Z, Zhang T, He Y, Zhang G. Generating progressive images from pathological transitions via diffusion model. *International Conference on Medical Image Computing and Computer-Assisted Intervention*. Springer; 2024:308–318.
245. Xu X, Kapse S, Gupta R, Prasanna P. Vit-dae: Transformer-driven diffusion autoencoder for histopathology image analysis. In: *International Conference on Medical Image Computing and Computer-Assisted Intervention*. Springer; 2023:66-76.
246. Pozzi M, Noei S, Robbi E, et al. Generating and evaluating synthetic data in digital pathology through diffusion models. *Sci Rep.* 2024;14(1):28435.
247. Shen Z, Cao M, Wang S, Zhang L, Wang Q. Cellgan: Conditional cervical cell synthesis for augmenting cytopathological image classification. In: *International Conference on Medical Image Computing and Computer-Assisted Intervention*. Springer; 2023:487-496.
248. Öttl M, Wilm F, Steenpass J, et al. Style-extracting diffusion models for semi-supervised histopathology segmentation. *Eur Conf Comput Vis.* 2024;2024:236–252.
249. Hou L, Agarwal A, Samaras D, Kurc TM, Gupta RR, Saltz JH. Robust histopathology image analysis: To label or to synthesize? In: *Proceedings of the IEEE/CVF Conference on Computer Vision and Pattern Recognition*. ; 2019:8533-8542.
250. Gong X, Chen S, Zhang B, Doermann D. Style consistent image generation for nuclei instance segmentation. In: *Proceedings of the IEEE/CVF Winter Conference on Applications of Computer Vision*. ; 2021:3994-4003.
251. Wang H, Xian M, Vakanski A, Shareef B. Sian: style-guided instance-adaptive normalization for multi-organ histopathology image synthesis. In: *2023 IEEE 20th International Symposium on Biomedical Imaging (ISBI)*. IEEE; 2023:1-5.
252. Xu M, Gupta S, Hu X, et al. TopoCellGen: Generating Histopathology Cell Topology with a Diffusion Model. *arXiv preprint arXiv:241206011*. Published online 2024.
253. Oh HJ, Jeong WK. Diffmix: Diffusion model-based data synthesis for nuclei segmentation and classification in imbalanced pathology image datasets. In: *International Conference on Medical Image Computing and Computer-Assisted Intervention*. Springer; 2023:337-345.
254. Yu X, Li G, Lou W, et al. Diffusion-based data augmentation for nuclei image segmentation. *International Conference on Medical Image Computing and Computer-Assisted Intervention*. Springer; 2023:592–602.

255. Min S, Oh HJ, Jeong WK. Co-synthesis of histopathology nuclei image-label pairs using a context-conditioned joint diffusion model. *Eur Conf Comput Vis.* 2024;2024:146–162.
256. Oh HJ, Jeong WK. Controllable and Efficient Multi-class Pathology Nuclei Data Augmentation Using Text-Conditioned Diffusion Models. *International Conference on Medical Image Computing and Computer-Assisted Intervention*. Springer; 2024:36–46.
257. Yellapragada S, Graikos A, Triaridis K, et al. ZoomLDM: Latent Diffusion Model for multi-scale image generation. *arXiv preprint arXiv:241116969*. Published online 2024.
258. Harb R, Pock T, Müller H. Diffusion-based generation of histopathological whole slide images at a gigapixel scale. In: *Proceedings of the IEEE/CVF Winter Conference on Applications of Computer Vision*. ; 2024:5131-5140.
259. Aversa M, Nobis G, Hägele M, et al. Diffinfinite: Large mask-image synthesis via parallel random patch diffusion in histopathology. *Adv Neural Inf Process Syst.* 2023;36:78126–78141.
260. Graikos A, Yellapragada S, Le MQ, et al. Learned representation-guided diffusion models for large-image generation. In: *Proceedings of the IEEE/CVF Conference on Computer Vision and Pattern Recognition*. ; 2024:8532-8542.
261. Le MQ, Graikos A, Yellapragada S, Gupta R, Saltz J, Samaras D. ∞-Brush: controllable large image synthesis with diffusion models in infinite dimensions. *Eur Conf Comput Vis.* 2024;2024:385–401.
262. Vaidya A, Chen RJ, Williamson DFK, et al. Demographic bias in misdiagnosis by computational pathology models. *Nat Med.* 2024;30(4):1174–1190.
263. Verma S, Rubin J. *Fairness definitions explained*. Software Fairness.; 2018:1–7.
264. AsilianBidgoli A, Rahnamayan S, Dehkharghanian T, Grami A, Tizhoosh HR. Bias reduction in representation of histopathology images using deep feature selection. *Sci Rep.* 2022;12(1):19994.
265. Nouyed MI, Hartley MA, Doretto G, Adjeroh DA. Efficient classification of histopathology images using highly imbalanced data. *Pattern Recognit.* 2025:160–175.
266. Chen RJ, Wang JJ, Williamson DFK, et al. Algorithmic fairness in artificial intelligence for medicine and healthcare. *Nat Biomed Eng.* 2023;7(6):719–742.
267. Jones C, Castro DC, De Sousa Ribeiro F, Oktay O, McCradden M, Glocker B. A causal perspective on dataset bias in machine learning for medical imaging. *Nat Mach Intell.* 2024;6(2):138–146.
268. Nan T, Ding Y, Quan H, et al. Establishing Causal Relationship Between Whole Slide Image Predictions and Diagnostic Evidence Subregions in Deep Learning. *arXiv preprint arXiv:240717157*. Published online 2024.
269. Tovino SA. The HIPAA privacy rule and the EU GDPR: illustrative comparisons. *Set Hall Law Rev.* 2016;47:973.
270. Nguyen DC, Pham QV, Pathirana PN, et al. Federated learning for smart healthcare: a survey. *ACM Comput Surv.* 2023;55(3):1–37.
271. Kaissis GA, Makowski MR, Rückert D, Braren RF. Secure, privacy-preserving and federated machine learning in medical imaging. *Nat Mach Intell.* 2020;2(6):305–311.
272. Uehara K, Murakawa M, Nosato H, Sakanashi H. Prototype-based interpretation of pathological image analysis by convolutional neural networks. *Pattern Recognit.* 2020:640–652.
273. Song AH, Chen RJ, Ding T, Williamson DFK, Jaume G, Mahmood F. Morphological prototyping for unsupervised slide representation learning in computational pathology. In: *Proceedings of the IEEE/CVF Conference on Computer Vision and Pattern Recognition*. ; 2024:11566-11578.
274. Pirovano A, Heuberger H, Berlemont S, Ladjal S, Bloch I. Improving Interpretability for Computer-Aided Diagnosis Tools on Whole Slide Imaging with Multiple Instance Learning and Gradient-Based Explanations. *Mach Intell Med Image Comput.* 2020:43–53.
275. Pirovano A, Heuberger H, Berlemont S, Ladjal S, Bloch I. Automatic feature selection for improved interpretability on whole slide imaging. *Mach Learn Knowl Extr.* 2021;3(1):243–262.
276. Hägele M, Seegerer P, Lapuschkin S, et al. Resolving challenges in deep learning-based analyses of histopathological images using explanation methods. *Sci Rep.* 2020;10(1):6423.
277. Casti P, Cardarelli S, Comes MC, et al. S3-VAE: a novel supervised-source-separation variational autoEncoder algorithm to discriminate tumor cell lines in time-lapse microscopy images. *Expert Syst Appl.* 2023;232:120861.
278. Hasan M, Hu X, Abousamra S, Prasanna P, Saltz J, Chen C. Semi-supervised contrastive VAE for disentanglement of digital pathology images. *International Conference on Medical Image Computing and Computer-Assisted Intervention*. Springer; 2024:459–469.
279. Jaume G, Pati P, Bozorgtabar B, et al. Quantifying explainers of graph neural networks in computational pathology. In: *Proceedings of the IEEE/CVF Conference on Computer Vision and Pattern Recognition*. ; 2021:8106-8116.
280. Jaume G, Pati P, Foncubierta-Rodriguez A, et al. Towards explainable graph representations in digital pathology. *arXiv preprint arXiv:200700311*. Published online 2020.
281. M G, V A, S MM, H M. Concept attribution: explaining CNN decisions to physicians. *Comput Biol Med.* 2020;123:103865.
282. Kapse S, Pati P, Das S, et al. Si-mil: Taming deep mil for self-interpretability in gigapixel histopathology. In: *Proceedings of the IEEE/CVF Conference on Computer Vision and Pattern Recognition*. ; 2024:11226-11237.
283. Javed SA, Juyal D, Padigela H, Taylor-Weiner A, Yu L, Prakash A. Additive MIL: intrinsically interpretable multiple instance learning for pathology. *Adv Neural Inf Process Syst.* 2022;35:20689–20702.
284. Wang J, Mao Y, Guan N, Xue CJ. SHAP-CAT: A interpretable multi-modal framework enhancing WSI classification via virtual staining and shapley-value-based multimodal fusion. *arXiv preprint arXiv:241001408*. Published online 2024.
285. Yan R, Sun Q, Jin C, et al. Shapley values-enabled progressive pseudo bag augmentation for whole-slide image classification. *IEEE Trans Med Imag.* 2025;44(1):588–597.
286. Wang X, Wang D, Yao Z, et al. Machine learning models for multiparametric glioma grading with quantitative result interpretations. *Front Neurosci.* 2019:12.
287. Lin T, Yu Z, Hu H, Xu Y, Chen CW. Interventional bag multi-instance learning on whole-slide pathological images. In: *Proceedings of the IEEE/CVF Conference on Computer Vision and Pattern Recognition*. ; 2023:19830-19839.
288. Chen K, Sun S, Zhao J. CaMIL: causal multiple instance learning for whole slide image classification. *Proc AAAI Conf Artif Intell.* 2024;38:1120–1128.
289. Qu J, Xiao X, Wei X, Qian X. A causality-inspired generalized model for automated pancreatic cancer diagnosis. *Med Image Anal.* 2024;94:103154.
290. Tian J, Yu H, Wang Y, Liang Z, Quan Y. A Dual-branch Self-supervised Learning Framework with Counterfactual Attention Learning for Histopathology Nuclei Segmentation. In: *2024 IEEE International Conference on Bioinformatics and Biomedicine (BIBM)*. IEEE; 2024:3762-3767.
291. Lin W, Zhuang Z, Yu L, Wang L. Boosting multiple instance learning models for whole slide image classification: a model-agnostic framework based on counterfactual inference. *Proc AAAI Conf Artif Intell.* 2024;38:3477–3485.
292. Thiagarajan JJ, Thopalli K, Rajan D, Turaga P. Training calibration-based counterfactual explainers for deep learning models in medical image analysis. *Sci Rep.* 2022;12(1):597.
293. Žigutytė L, Lenz T, Han T, et al. Counterfactual Diffusion Models for Mechanistic Explainability of Artificial Intelligence Models in Pathology. bioRxiv. Published online. 2025:2010–2024.
294. Collins GS, Moons KGM, Dhiman P, et al. TRIPOD.AI statement: updated guidance for reporting clinical prediction models that use regression or machine learning methods. *BMJ.* 2024;385:e078378.
295. Norgeot B, Quer G, Beaulieu-Jones BK, et al. Minimum information about clinical artificial intelligence modeling: the MI-CLAIM checklist. *Nat Med.* 2020;26(9):1320–1324.
296. Luo W, Phung D, Tran T, et al. Guidelines for developing and reporting machine learning predictive models in biomedical research: a multidisciplinary view. *J Med Internet Res.* 2016;18(12):e5870.
297. Warraich HJ, Tazbaz T, Califf RM. FDA perspective on the regulation of artificial intelligence in health care and biomedicine. *JAMA.* 2025;333(3):241–247.
298. Aboy M, Minssen T, Vayena E. Navigating the EU AI act: implications for regulated digital medical products. *npj Digit Med.* 2024;7(1):1–6.
299. Bera K, Schalper KA, Rimm DL, Velcheti V, Madabhushi A. Artificial intelligence in digital pathology — new tools for diagnosis and precision oncology. *Nat Rev Clin Oncol.* 2019;16(11):703–715.
300. Johnson DB, Bordeaux J, Kim JY, et al. Quantitative spatial profiling of PD-1/PD-L1 interaction and HLA-DR/IDO-1 predicts improved outcomes of anti–PD–1 therapies in metastatic melanoma. *Clin Cancer Res.* 2018;24(21):5250–5260.

301. Plaks V, Kong N, Werb Z. The cancer stem cell niche: how essential is the niche in regulating stemness of tumor cells? *Cell Stem Cell.* 2015;16(3):225–238.
302. Pribluda A, De La Cruz CC, Jackson EL. Intratumoral Heterogeneity: From Diversity Comes Resistance. *Clin Cancer Res.* 2015;21(13):2916–2923.
303. Wang A, Zhang Q, Han Y, et al. A novel deep learning-based 3D cell segmentation framework for future image-based disease detection. *Sci Rep.* 2022;12(1):342.
304. Liu JTC, Glaser AK, Bera K, et al. Harnessing non-destructive 3D pathology. *Nat Biomed Eng.* 2021;5(3):203–218.
305. Bressan D, Battistoni G, Hannon GJ. The dawn of spatial omics. *Science.* 2023;381(6657):eabq4964.
306. Marconato L, Palla G, Yamauchi KA, et al. SpatialData: an open and universal data framework for spatial omics. *Nat Methods.* 2024;22(1):58–62.
307. Azher ZL, Fatemi M, Lu Y, et al. Spatial omics driven crossmodal pretraining applied to graph-based deep learning for cancer pathology analysis. *Biocomputing.* 2023;2024:464–476.
308. Lee G, Kim S, Kim J, Yun SY. MEDIAR: harmony of data-centric and model-centric for multi-modality microscopy. *arXiv preprint arXiv:221203465*. Published online 2022.